Chair of Applied Mechanics
Department of Mechanical Engineering
Technical University of Munich

ΠΙΠΙ

On the Experimental Characterization and Numerical Modeling of a Nonlinear Bolted Contact

Semester Thesis

at the Department of Mechanical Engineering of the Technical University of Munich

Supervisor	Prof. dr.ir. Daniel J. Rixen Chair of Applied Mechanics
Advisor	Francesco Trainotti, M.Sc. Chair of Applied Mechanics
Submitted by	Sebastian Sterr Oberauerstr. 6 81377 München
Submitted on	March 28, 2022 in Garching bei München

Abstract

In this semester thesis a QSMA routine based on the theory of Allen et al. [1] is implemented using Python and the commercial finite element software Abaqus. The routine is applied to a high fidelity FE model of a Brake-Reuß beam variant with a single bolt and Coulomb friction modelled at the interface between the beams. The QSMA results are compared with experimental data obtained by impact hammer testing of the physical structure. In the course of this, the validity of the routine is examined and the influence of certain model parameter and routine settings on the QSMA results are investigated. The focus of this work is on the specific implementation of the routine and on investigating the problem of unstable QSMA results due to rigid body modes when the system is analyzed in the free-free configuration.

Zusammenfassung

In dieser Semesterarbeit wird eine QSMA-Routine basierend auf der Theorie von Allen et al. [1] mit Python und der kommerziellen Finite-Elemente-Software Abaqus implementiert. Die Routine wird auf ein „High-Fidelity" FE-Modell einer Brake-Reuß-Träger-Variante mit einer einzelnen Schraube und Coulomb-Reibung an der Schnittstelle zwischen den Trägern angewandt. Die QSMA-Ergebnisse werden mit experimentellen Daten verglichen, die durch Schlaghammerversuche mit der physischen Struktur gewonnen wurden. Im Zuge dessen wird die Gültigkeit der Routine überprüft und der Einfluss bestimmter Modellparameter auf die QSMA-Ergebnisse untersucht. Der Schwerpunkt dieser Arbeit liegt auf der spezifischen Implementierung der Routine und auf der Untersuchung des Problems der instabilen QSMA-Ergebnisse aufgrund von Starrkörpermoden, wenn das System ohne Randbedingungen analysiert wird.

Contents

Chapter 1

Introduction

Finite element analysis (FEA) is a central part of the design process of structural components in today's development processes. Powerful software tools such as Abaqus allow for a variety of different FEA analyses, which can be used to simulate the mechanical behaviour of the structure under investigation. With today's FEA methods, it is possible to accurately determine the dynamic response in terms of the inertia, stiffness, and damping properties of a single solid structure, especially when the problem is linear. However, most structures consist of several parts fastened together by bolts. Friction in the joints causes nonlinear damping, which makes the prediction of the overall damping properties of the assembled structure very complex [8, 16].

The nonlinear damping coming from the joints originates from slip at the contact interface both at microscopic and macroscopic levels [8]. Per cycle of vibration, the forces acting on the joints cause some areas within the contact to slip relative to each other while other areas remain stuck. For bolted joints, it is distinguished between micro-slip and macro-slip as the two types of motion during vibration. A joint is in the micro-slip regime if some areas of the contact interface slip while others remain stuck. As the load on the joint increases, macro-slip occurs, where the entire interface slips [8, 16].

To accurately represent micro-slip friction, the finite element model usually requires a much higher mesh density in the region of the joint than in the rest of the structure. Meshing the contact surfaces with sufficient resolution leads to very expensive simulations if the static response is to be calculated, and to completely infeasible simulations if the dynamic response over many vibration cycles is desired [8, 10]. Even advanced simplification approaches to speed up the computation such as the as a model-order reduction of the linear domain away from the joint area cannot change this fact [16]. In addition, the energy lost to damping in a contact simulation is usually 2-4 orders of magnitude smaller than the elastic energy. Therefore, this type of analysis requires much higher accuracy than, for example, stress analyses [8]. Due to the aforementioned issues, industry typically relies on testing physical prototypes of structures containing bolted joints, which often also involves significant cost [4, 8].

One approach to overcome the problem of the computational expense in dynamic simulations originates from a paper by Festjens et al. [6]. The authors' approach is to treat the joint as a quasi-static subcomponent in an otherwise linear, overall dynamic model [16]. Allen et al. [1] have extended the approach of Festjens et al. [6] and presented a fast and efficient computational method for extracting the amplitude-dependent modal properties from a finite element model. This method is also referred to as "quasi-static modal analysis" (QSMA) and allows the effective natural frequency and modal damping ratio to be extracted from a nonlinear static analysis by imposing a quasi-static load on the model that excites only a single mode of the linearized structure. The QSMA method is a promising approach to over-

come the lack of modeling capabilities to capture nonlinearities of joints in an efficient and industry applicable way [8]. However, the method is still part of current research where the opportunities and limitations of the quasi-static modal analysis method are investigated.

The goal of this work is to develop a QSMA routine based on the theory of Allen et al. [1], using Python and the commercial finite element software Abaqus. The routine is applied to a high fidelity model of a Brake-Reuß beam variant with a single bolt and Coloumb friction modelled at the interface between the beams. The functionality of the routine is then validated by comparing its results with data from impact hammer tests of the test structure. Furthermore, the influence of certain model parameters and routine settings on the QSMA results is investigated.
Due to the non-trivial problems encountered regarding the interface between the Python routine and Abaqus, a great deal of attention was paid to the implementation of the routine and its logic regarding the extraction and utilisation of the simulation data. Another focus was set on the investigation of the problem of unstable QSMA results due to the influence of the rigid body modes when analyzing the system in the free-free configuration.

The thesis is structured as follows: In chapter 2, a short overview of current research on the quasi-static modal analysis is given and the theory of QSMA as implemented in the routine is reviewed briefly. General aspects, the basic functionality and the practical implementation of the routine are explained in chapter 3. In chapter 4, the experimental investigation of the test structure used to validate the QSMA routine is discussed. In the course of this, the design of the test structure is described and the experiments for determining the preload-torque relationship and the impact hammer tests are covered. In Chapter 5, the results of the QSMA routine are evaluated and compared with the results from the impact hammer tests. General information about the creation of the FE model of the test structure is given. The QSMA results of the structure in free-free configuration are then evaluated and the problems encountered in terms of stability are addressed. The second part of this chapter presents the QSMA results from a parameter study of the test structure with boundary conditions. The obtained results are summarised and discussed in chapter 5.

Chapter 2

Literature Review and Theoretical Framework

In the following section, some academic work related to current research on QSMA is presented. Then the theory of quasi-static modal analysis as implemented in this work is described.

2.1 Research on the Topic QSMA

The work of Festjens et al. [6] represents the groundwork for the QSMA method later further developed by Allen et al. [1]. The authors present a method of extracting the natural frequency and damping of a structure by treating the joint as a quasi-static subcomponent in an otherwise linear, dynamic global model [16]. Their concept is based on the idea of using the modes of the equivalent linear structure as boundary conditions on a detailed, nonlinear quasi-static model of the region around the joints. The modal properties are determined by an iterative procedure in which the boundary conditions are updated for each loading cycle [6].

Allen et al. [1] later presented a derivation of the method mentioned above, which is referred to as the quasi-static modal analysis (QSMA). The QSMA method is in comparison to the approach from Festjens et al., faster and more computational efficient, because it does not seek to update the mode shape with displacement amplitude [1]. The theoretical framework of this method and the differences between the two approaches are explained in section 2.2.

In the paper by Wall et al. [16] a detailed finite element model of the S4 beam is analysed with a Coulomb friction law assigned at the interfaces between the parts using QSMA. The authors use Abaqus as the FE package. The obtained amplitude-dependent damping and natural frequency curves for a single mode are investigated and compared with experimental measurements. The influence of different parameters such as the convergence tolerances, the preload and the surface flatness on the QSMA results is investigated. A parameter study revealed, that the model and the measurements could be brought into agreement but only with highly adjusted model parameters.

In the work of Jewell et al. [8], the quasi-static modal analysis is applied to a 2D and a 3D FE model of a cantilever beam and to a finite element model of the S4 beam. In all investigations, the joint region is modelled with a detailed geometry, contact pressure and Coulomb friction at the part interface. The effects of certain model parameters and solver settings such as the mesh density or the solver tolerance on the ability to predict the non-linear behaviour are evaluated for the different models investigated. All simulations were performed using Abaqus. Both analyses of the 2D and 3D models produced reasonable re-

sults. The analysis of the S4 beam was not yet predictive, but according to the authors, some aspects of the model matched the measurements quite well.

Lacayo et al. [10] present a modified QSMA method which allows to analyse unconstrained models. The authors apply this method to analyse a finite element model of a Brake-Reuß beam with three bolts. The obtained QSMA results are used to update a set of Iwan joint parameters so that the natural frequency and damping ratio curves match those from measurements on an experimental beam. It was shown that the updated model is capable of capturing with good accuracy the effects of modal coupling seen in the impact response of the beam.

Lengger et al. [11] have applied the QSMA analysis to the Tribomechadynamics Benchmark System. The authors address the asymmetric modal force-deflection behaviour of the structure by using several modal loading curves to determine the amplitude-dependent modal properties. Their QSMA framework, implemented with Abaqus and Python, is therefore different from the standard implementation [1], which assumes Masing's rules. The parameter study is performed using an FE model in which the bolt shanks are modelled with Timoshenko beam elements (B31) connected to both jointed parts by multipoint constraints (MPC). The investigations have shown that the consideration of the asymmetrical modal force-deflection behaviour is necessary for the application case, but is associated with a high computational effort.

Jewell et al., Lacayo et al. and Wall et al. achieved useful results with their QSMA analyses. However, it turns out that the structures have to be meshed with a reasonable accuracy in order to capture the micro-slip, and thus achieve a certain accuracy of the results. This has a significant impact on the computational costs [16]. To address this, Zare et al. [18] presented a quasi-static algorithm that accelerates the analysis of 2D and 3D problems. This algorithm uses static reduction along with a new numerical method which is a hybrid between Block-Gauss-Seidl and Newton-Rhapson. The nonlinear contact problem is solved in Matlab and their algorithm is implemented for structures where the joint is modelled in detail [16]. The algorithm was found to provide a large reduction in computation time compared to using Abaqus and the standard QSMA.

2.2   Theory of the Quasi-Static Modal Analysis

In this work, the QSMA analysis of Allen et al. [1] is implemented. By using this method, it is possible to extract the effective natural frequency and modal damping ratio from a nonlinear static analysis by imposing a quasi-static load on the model that excites only a single mode of the linearised structure. The theory of the quasi-static modal analysis is briefly explained below and is based on [1] and [16].

The equation of motion for an otherwise linear structure that contains localised nonlinearities due to joints can be written as follows:

$$M\ddot{x} + C\dot{x} + Kx + f_J(x, \theta) = f_{ext}(t) \tag{2.1}$$

The matrices M, C and K are the mass, the damping and stiffness matrices of the system. x, $\dot{x}$ and $\ddot{x}$ are the displacement, velocity and acceleration vectors. The vector f_J represents the internal nonlinear forces due to a joint model containing internal sliders. These nonlinearities are assumed to depend only on the displacement and the vector θ, which captures the

internal state (slip or stick) of each slider element [1, 16].

For small vibrations, one can define a linear system that approximates the response about some equilibrium. This is like replacing the joints with springs equivalent to the preloaded stiffness of the joints. The term $\nabla f_J|_{x=0}$ denotes the Jacobian of the nonlinear forces at the equilibrium state $x = 0$, which corresponds to the preloaded state. The corresponding equation of motion then becomes:

$$M\ddot{x} + C\dot{x} + (K + \nabla f_J|_{x=0})\,x = f_{ext}(t) \tag{2.2}$$

For this linear system, an eigenvalue problem can be solved to find the systems mass-normalized mode shapes φ_r:

$$([K + \nabla f_J|_{x=0}] - \lambda M)\,\varphi_r = 0 \tag{2.3}$$

From this point on, the methods of Festjens et al. and Allen et al. differ. Festjens et al. [6] divide the structures into two substructures, a nonlinear domain that includes the joint(s) and a linear domain that corresponds to the rest of the structure. This partitioning leads to coupled equations, which are derived from eq. (2.1) [16]. The assumed deformation of the linear domain (in the shape of the mode of interest) provides the boundary conditions for the nonlinear static solution on the joint domain. However, since the deformation of the entire structure changes when the joint slips (and its stiffness decreases), they had to use an iterative procedure to adjust the boundary conditions [10]. In contrast, Allen et al. [1] do not divide the structure into different substructures, but analyze it as an entire nonlinear domain. Applying only a force rather than a displacement, allows the structure to adjust quasi-statically in response to small changes in stiffness near the joint. Therefore, this method does not require updating the mode shape with the displacement amplitude, as it was done by Festjens et al. [6]. As a results, only a single nonlinear static analysis for the mode under investigation is needed [10]. Following their approach, the mode of interest r is excited with a force applied over the entire structure in the shape of that linear mode by solving the following quasi-static problem, where the scalar α is the load amplitude:

$$Kx + f_J(x, \theta) = M\varphi_r\alpha \tag{2.4}$$

The quasi-static response $x(\alpha)$ of the structure for a given load amplitude is determined using a finite element package, Abaqus in this work. The resulting response is then mapped to the mode of interest r using:

$$q_r(\alpha) = \varphi_r^T M x(\alpha) \tag{2.5}$$

The solving of the quasi-static problem as well as the corresponding mapping of the response is performed for different load amplitudes increasing from an unloaded state to a certain maximum load. The obtained data, in form of the modal force $f_r(\alpha) = \varphi_r^T M \varphi_r \alpha = \alpha$ versus the modal displacement q_r, represents the initial loading of the structure [1]. This so-called backbone curve is then used to construct the forward part (eq. (2.6a)) and the backward part (eq. (2.6b)) of the full hysteresis curve by using Masing's rules, as shown in fig. 2.1 [6, 16]:

$$\hat{f}_1(q_r) = 2f_r\left(\frac{q_r + q_r(\alpha)}{2}\right) - \alpha \tag{2.6a}$$

$$\hat{f}_2(q_r) = \alpha - 2f_r\left(\frac{q_r(\alpha) - q_r}{2}\right) \tag{2.6b}$$

The secant of the hysteresis curve can then be used to estimate the instantaneous natural frequency of the mode of interest r:

$$\omega_r(\alpha) \triangleq \sqrt{\frac{\alpha}{q_r(\alpha)}} \tag{2.7}$$

The area enclosed by the full hysteresis curve is the energy dissipated per each cycle of vibration:

$$
\begin{aligned}
D_r(\alpha) &= \int_{-q_r(\alpha)}^{q_r(\alpha)} \left(\hat{f}_1(q_r) - \hat{f}_2(q_r) \right) dq_r \\
&= 2 \int_{-q_r(\alpha)}^{q_r(\alpha)} \left(f_r \left(\frac{q_r + q_r(\alpha)}{2} \right) + f_r \left(\frac{q_r(\alpha) - q_r}{2} \right) - \alpha \right) dq_r
\end{aligned}
\tag{2.8}
$$

Here α denotes the constant maximum load at the level of interest ($\alpha = \alpha_{max} \rightarrow q_r(\alpha) = q_{max}$) and f_r is a function of the displacement q_r. The practical evaluation of the integral, as it was done in this work, is described in section 3.2.2.

Based on the relationship between the energy dissipated per vibration cycle and the damping ratio, the effective damping ratio can be determined by analogy with a linear system:

$$\zeta_r(\alpha) = \frac{D_r(\alpha)}{2\pi \left(q_r(\alpha) \omega_r(\alpha) \right)^2} \tag{2.9}$$

Since in a QSMA analysis the mode r under investigation is not changed, the notation in the formulas above $..._r$ will be omitted in the following sections of this thesis for better clarity.
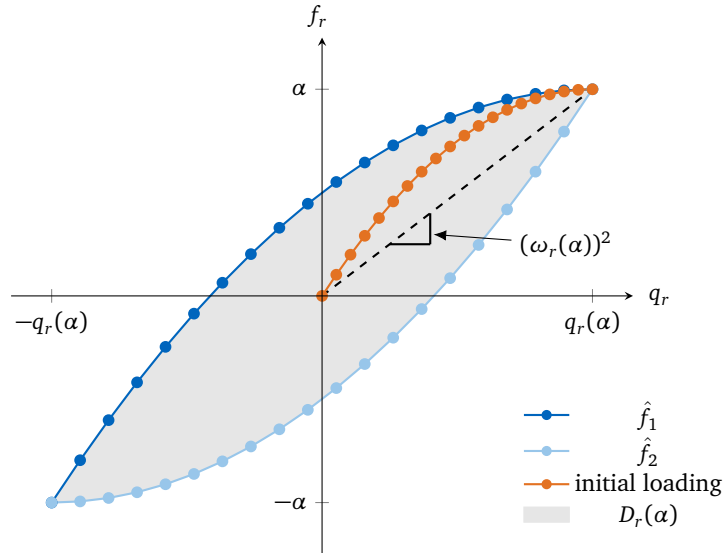

Figure 2.1: An example an initial loading curve and a full hysteresis curve of the last modal force - modal displacement sample pair of the analysis, derived from Masing's rules. The damping in typical structures is very light, so the hysteresis curve may show much less dissipation than the one shown here.

Chapter 3

QSMA Implementation

The following chapter describes how the concept of QSMA was practically implemented in a Python routine. First, the basic functionality of the routine is explained and general aspects such as the hardware and software used are described. Then, a detailed documentation of the implemented functions is given, focusing on the special features and extensions of the routine.

3.1 Basic Functionality and General Aspects of the QSMA Routine

Basic Functionality of the Routine

Considering QSMA from a practical point of view, the method can be divided into two analysis parts, which are used to determine the amplitude-dependent natural frequencies and damping ratios of a jointed system. Both the modal analysis part and the subsequent static analysis part consist of a sequence of two main analysis steps. In step 1 of the modal analysis part, the individual components of the structure are jointed by applying some preload. In step 2, a modal analysis of the jointed system is performed. In step 1 of the static analysis part, the individual components of the structure are jointed in the same way as in the modal analysis part. In step 2, a static analysis is conducted in which the preloaded and joined system is excited with a force proportional to the properties determined in the modal analysis part. Based on these conceptual considerations, the QSMA routine was developed. The two main analysis parts were thereby embedded in a sequence of operations to solve the task. In the following, the general function of the routine is described on the basis of the program flow chart as shown in fig. 3.1.

1. Before the routine is able to run, certain variables and settings have to be specified by the user. This is illustrated by the Input/Output block in the flow chart. A description of the variables and settings is given in the next section.

2. The following grey process blocks represent a group of functions, which are used for the general setup of the routine. With `q = np.zeros(len(alpha))` the empty displacement array is created based on the user specified load amplitude array `alpha`. The `wd_setup()` function is then used to create a new working directory for the project. Afterwards, the modal input file is copied into this project directory by using the `shutil.copy2()` function. Then, the working directory is changed with `os.chdir()`.

3. The blue process blocks represent the model analysis and evaluation part of the routine. The `output()` function is used to add, if not already included, necessary commands to the modal analysis .inp file so that Abaqus outputs the mass and stiffness matrix as

well as the modes. The job is then submitted to Abaqus by calling the `run_abaqus()` function. After Abaqus has finished, the systems matrices are obtained with the use of the `mtx_read_and_change()` function. The mass and stiffness matrices are then used to calculate a certain number of lowest natural frequencies and the corresponding modes with the `eigenproblem()` function. The calculated mode, which is the subject of the QSMA analysis, is then extracted from these eigensolutions. Subsequently, the corresponding mode from the .dat file of the modal analysis is retrieved using the `mode_from_dat()` function. The transformation matrix between the two modes, which have different dimensions and a different entry arrangement, is then determined using the `mapping()` function.

4. The green process blocks represent the static analysis and evaluation part of the routine. A static analysis is performed for all user-defined load amplitudes and thus entries of `alpha`. For each analysis loop, first the current load amplitude is selected by `a = alpha[i]`, then the name of the static job and the corresponding .inp file name is set. After that, the .inp file of the static analysis is created with the use of the `write_static_inp()` function. To obtain the force applied over the entire structure in the shape of the mode of interest for a certain load amplitude, the `external_force()` function is internally called. If the user opts to exclude a certain part instance (by default the bolt assembly) from loading, the `part_instance_nodes()` function is also called in the course of creating the static .inp file. The created .inp file of the static job is then submitted to Abaqus by calling the `run_abaqus()` function. After completion, the modal displacement `q` is obtained from the quasi-static response of the structure by the use of the `qs_response()` function. For this, the nodal displacement resulting from the Abaqus analysis of the simulation, is extracted from the corresponding .dat file by calling the `u_from_dat()` function.

5. The last grey process blocks are also categorised as general setup functions. After the routine has finished evaluating the static job with the last load amplitude, the function `save_results()` is used to save the array data of the different load amplitudes `alpha` and the corresponding modal displacement array data `q` of the whole QSMA analysis into two CSV files. Before the QSMA routine finishes its execution, the working directory is changed back with `os.chdir()` and the load amplitude array as well as the modal displacement array are returned with `return alpha, q`.

General Requirements and Setup of the Routine

The QSMA routine requires a specific Abaqus input file, referred to as "modal input file" from the FE model of the test structure to be analyzed. This .inp file must contain a static preload step followed by a modal analysis step in which the calculation of a specified number of the lowest eigenvalues is required. In the context of this work, the routine is used in a setup where a single bolt is preloaded and the first ten lowest eigenvalues are calculated. The modal input file has to be placed in the same working directory as the QSMA.py script in order to make the routine run. The modal input file can be generated using the Abaqus CAE GUI. For this purpose, a job of the test structure model must be created according to the mentioned specifications and the corresponding .inp file must be written. It is very important that the modal input file is generated from a model with the attribute "do not use parts and assemblies in input files" activated (In the Abaqus CAE GUI: right click on model → edit Attributes → tick corresponding box). This setting leads to a continuous and therefore non redundant numbering of the nodes of the assembled structure, which is required for a working routine.

Prior to starting the QSMA routine, certain variables and settings of the analysis have to be specified in the main `QSMA()` function. This includes the definition of a project name (`project_name`), the selection of the investigated mode (`mode_nr`), the specification of the load amplitude array (`alpha`) and the possible activation of a stabilization (`stabilize`) or the removal of the bolt assembly (`assembly_remove`). Due to the implementation of the data extraction from Abaqus analyses, it is only possible to extract all modes except the last and therefore highest of the specified number within the modal analysis step. This has to be taking into account for the selection of `mode_nr`. The exact reason for this is explained in the documentation of the `u_from_dat()` function. When specifying the load amplitude array (`alpha`), care must be taken that the first entry must be equal to zero. This is important because the resulting displacement of the unloaded structure resembles a simulation offset which is removed from the QSMA results with actual loading.

The user can specify with `stabilize = True` that the automatic stabilization of Abaqus is used during the static analysis. As a default, allsdtol = 0.05 is used to specifiy the stabilization. It is important to note that if stabilization is to be used in the QSMA analysis, the preload step in the modal input file must contain the same commands as the routine adds to the static input file. More detailed information about the stabilization is provided in section 5.2.4. If the user wants to exclude the bolt assembly from loading, the `assembly_remove` parameter must be set to `True`. The exclusion is implemented in such a way that the nodes corresponding to the part instance "bolt assembly-1" are excluded from loading. The use of this feature is explained in section 5.3.6.

Hardware and Software Requirements

In the following, the hardware and software specifications of the resources used to develop and run the QSMA routine are given. For all conducted simulations, a Windows desktop computer with an Intel Xeon, 3.50 Ghz, 4 core CPU and 16 GB RAM was used. All models were solved utilising a single core and without parallelization. Is is recommended to use a computer with at least the same hardware specifications because the solving of even small models was very demanding regarding the necessary memory. The complete QSMA routine is programmed in Python (Python 3.8). Anaconda in the 64-bit version and the included Sypder IDE (version 5.1.5) were used for the code development and to run the routine. Abaqus CAE 2020 was used as FE package with a teaching licence. It was taken care, to program the routine as efficient as possible regarding the required memory used. This included for example, the usage of the mass and stiffness matrices only in sparse format or the avoidance of loading complete text files into memory when extracting information.
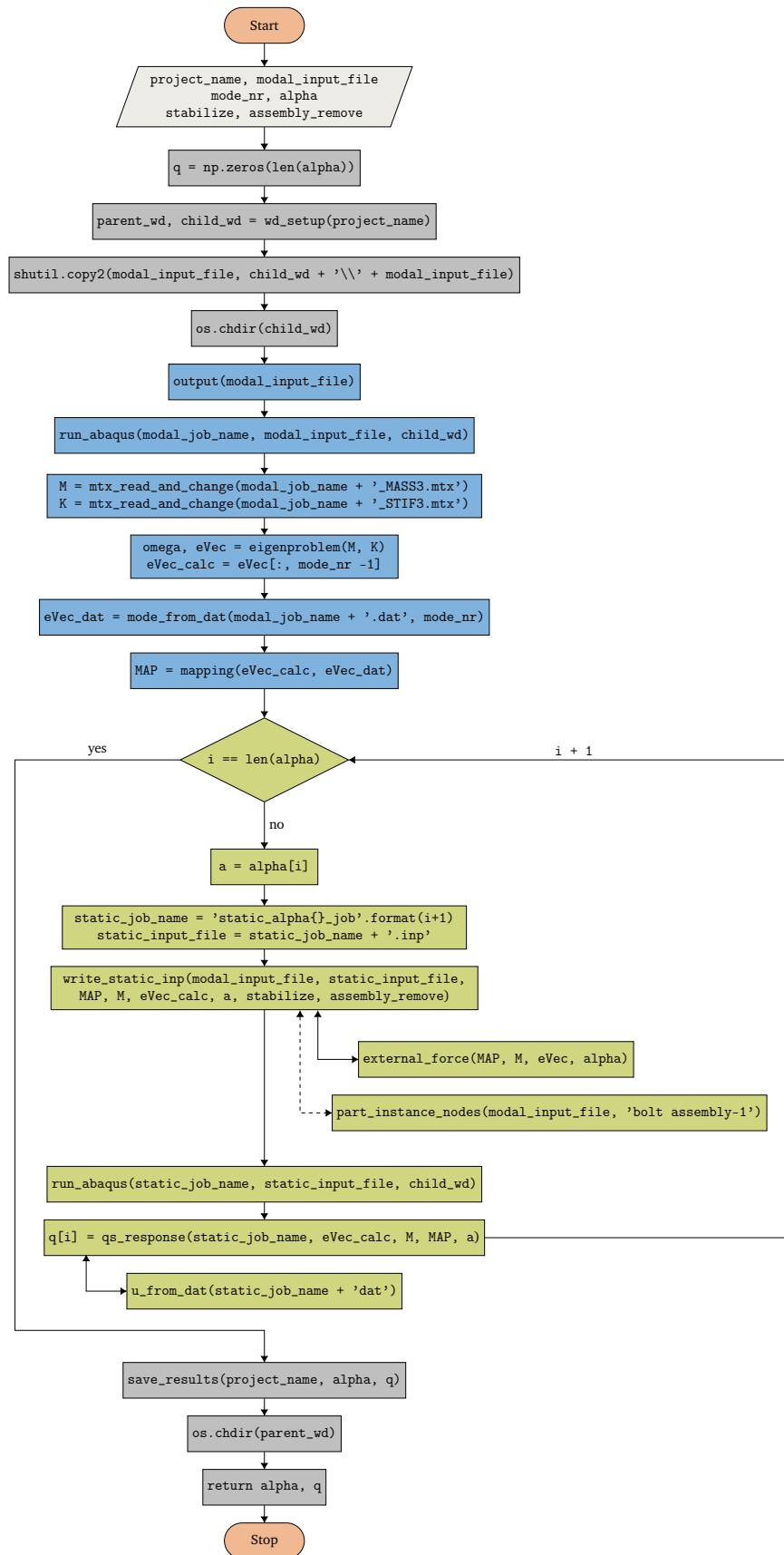
Figure 3.1: Flowchart of the QSMA routine - color coding according to the different parts of the routine

3.2 Practical Implementation of the QSMA Routine

The following section contains the documentation of all self-programmed functions used for the QSMA routine. In addition to the functions included in the algorithm (see fig. 3.1), the implementation of the `evaluation()` function is described. This function is used to evaluate the obtained QSMA results, but is not part of the general algorithm and must be called separately.

3.2.1 Documentation of the QSMA Routine Functions

`wd_setup(project_name)`   The `wd_setup()` function is used to create a new working directory (folder) called `project_name` in the current working directory. All files generated by the QSMA routine will be stored in this directory.

`output(filename)`   The `output()` function is used in the course of the QSMA routine to modify the input file of the modal analysis. It checks if the Abaqus input file - `filename`, includes the necessary commands to output the nodal displacement U in the .dat file of the analysis as well as the mass and stiffness matrices, both in coordinate format, in separate .mtx files. If the necessary commands aren't already present, an intermediate file, called `mod_file.inp`, is created. This file consists of the original input file except the command "`*End Step`" and the appended output commands with the "`*End Step`" command in the last line. After that, the original input file is removed and the intermediate file is renamed as the original one. The procedure of creating an intermediate input file is necessary because it is not possible in python to insert a text section into an existing text file.

`run_abaqus(job_name, inp_file_name, wd)`   The `run_abaqus()` function is used to create and submit a job to Abaqus based on the `inp_file_name` and other additional specifications. Calling `run_abaqus()` creates a python script named `run_job_name.py`. This script contains commands for the creation of a job named `job_name` based on the input file called `inp_file_name` and additional specifications for the submission of this job like the number of CPU cores used. The `os.system()` module is used to run Abaqus/CAE without the graphical user interface (GUI). Abaqus executes the commands specified in the `run_job_name.py` script and exits upon completion, allowing the routine to continue.

`mtx_read_and_change(filename)`   The function `mtx_read_and_change()` is used to create and modify the mass and stiffness matrices from the .mtx files generated by Abaqus in the course of the modal analysis. The commands added by the `output()` function specify that the matrix data is stored in coordinate format. Thus, each line in the .mtx file specifies a single matrix entry that is non-zero or located on the diagonal and is equal to zero. The first entry of each line specifies the row, the second specifies the column and the third specifies the value of the matrix entry. The function is setup to determine the size of the generated matrices based on the row or column entry of the last line in the .mtx file (row and column are the same due to symmetry). On this basis, the corresponding sparse matrix is created. In the course of that, the algorithm checks whether the corresponding .mtx file contains leading zeros on the diagonal and, if so, truncates them from the resulting matrix in sparse format. The reason for this is explained below.

Tests showed, that the generated mass and stiffness matrices could not be used directly in the QSMA routine without the truncation. The dimensions of the systems matrices did not match

the "number of nodes defined by the user" times three and the calculation of the eigensolutions was either wrong (compared to the ones from the .dat file) or not possible at all (due to singularity). This problem can be seen in context of the influence of the connections and interactions between the different parts in the FE model assembly. In the context of this work, two different contact properties are used. The contact at the interface of the jointed beams is defined as an interaction with Coulomb friction. It is specified by a penalty formulation in the horizontal direction and a linear pressure-overclosure relationship in the tangential direction. In the following it will be referred to as "interaction". The detailed specifications of the corresponding coefficients can be found in section 5.1. The contact between the bolt assembly and the two beam surfaces is defined as a "tie" connection. To further investigate the effects of these contact properties on the matrix creation, a small test model with a small number of total variables was created and investigated for different settings. To test the influence of the interaction contact formulation, an assembly of two "beam" parts connected with the interaction property as contact was investigated. In order to test the influence of the tie constraint, the model was then extended by an additional third part which was tied to the top of one of the "beam" parts, as shown in fig. 3.2. Both assemblies were tested in
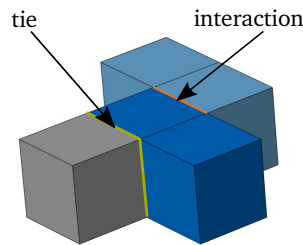

Figure 3.2: Small test model with 32 nodes defined by the user. Both beam parts are coloured blue and the additional part is coloured grey.

a free-free configuration without any boundary conditions. A modal analysis was conducted and the mass and stiffness matrices were generated. The information of the problem size as well as the eigensolutions provided by Abaqus in the respective .dat file, were compared to the calculated eigensolutions obtained by the `eigenproblem()` function. Since both models have small mass matrices with a simple structure containing only entries on the diagonal, the insights were obtained based on studies of these matrices.

The generated mass matrix of the interaction model (only the two "beam" parts) has a total number of 84 entries, all positioned on the diagonal of the matrix. The first 12 entries are zero followed by 72 non zero entries. The number of degrees of freedom related to the nodes which are defined by the user (24) results in 72, what suggests that the non zero matrix entries belong to these nodes. It is assumed, that the leading zero entries in the matrices belong to a certain number of internal variables generated by Abaqus like degrees of freedom of internal nodes or Lagrange multiplier variables. When the leading zero entries are truncated from the mass and the stiffness matrix, the calculated eigensolutions match the ones from Abaqus. The inclusion of the additional third part of the assembly (interaction + tie model), leads to 32 nodes defined by the user and an associated mass matrix with a total number of 96 entries which are also all arranged on the diagonal. The first 12 entries are still zero, followed by 84 entries that are predominantly non-zero. It is assumed, that the intervening zero entries are due to the tie constraint. No further investigation was done on the connection of the tie constraint and these intervening zeros, as it is found sufficient to truncate the leading zero entries from the matrices, as in the previously mentioned interaction model, to obtain matching eigensolutions.

In conclusion, it was found that the simple step of truncating the leading zero entries in the mass and stiffness matrices results in correct system matrices and thus correct eigensolutions. The results were verified on the actual FE models used in the course of this work.

mode_from_dat(datfile, mode_nr) This function is used to extract the mode corresponding to a specific `mode_nr` from the .dat file (`datfile`) of the modal analysis. This requires that the specific command to output the nodal displacement U is included in the corresponding .inp file of the analysis (see `output()` function). In that case, Abaqus lists the nodal displacement of all user defined nodes for a specified number of eigensolutions (default is ten) in the .dat file. The data for each mode is arranged in a table which is separated from the others by the heading of the following "eigenvalue nr". In such a table, one line includes the node number and the corresponding displacements in all three dimensions (`node_number U1 U2 U3`). The heading of the respective following "eigenvalue nr" is used to define the section in which the displacement data is extracted from the file. Since such a heading is not included for the last output mode, it cannot be extracted and results in an error. The extracted data for the corresponding `mode_nr` is returned in the so called `eVec` array. In this array, all displacement entries for each user defined node are listed one below the other.

u_from_dat(datfile) The `u_from_dat()` function of the QSMA routine is used to extract the quasi-static response of the structure from the `datfile` of a certain static analysis with a specific load amplitude. The necessary command to output the nodal displacement U in the .dat file of the corresponding `static_input_file`, is written to the .inp file of the analysis within the `write_static_inp()` function. Abaqus writes the nodal displacement of all user-defined nodes to the .dat file for each specified time increment in the same way as described in the `mode_from_dat()` function paragraph. The data for each increment is also arranged in tables separated by a heading of the following increment. The `u_from_dat()` function is set up to extract the nodal displacement and thus the quasi-static response of the structure from the last increment within the static step of the analysis. The retrieved displacement data is returned in the array u, which lists all displacement entries for each user-defined node, one below the other.

eigenproblem(M, K, n = 10, shift = 0) The function `eigenproblem()` is used to obtain the natural vibration frequencies and the corresponding mode shapes of the structure by solving the eigenproblem of the homogeneous linear system. For this purpose, the `linalg.eigs` solver of the `scipy.sparse` package is used with the structures mass - M and stiffness matrix - K. By default, the first ten lowest natural frequencies and the corresponding modes are calculated (`n = 10`) and no shift is applied (`shift = 0`). The determined natural frequencies in Hz are ordered in an ascending way in the `omega` array. The corresponding modes are returned in the `eVec` array and are sorted in the same way.

mapping(EV_calc, EV_dat) For the implementation of the QSMA routine, it is necessary to perform certain intermediate computations based on the obtained results from the Abaqus analyses. This includes the calculation of the external force which is applied on the entire structure for different amplitudes `alpha` as well as the corresponding calculation of the the modal displacement q based on the structure's quasi-static response (see section 2.2). For both of these calculations, it is necessary to multiply either an eigenvector or the quasi-static response vector with the mass matrix.
The obvious approach of using the eigenvector retrieved from the .dat file of the modal analysis for the calculation of the external force led to the problem that its dimensions do not

match those of the mass matrix in both forms (with and without leading zeros on the diagonal). Thus, no calculation is possible. It was found that the natural frequencies obtained by calling the `eigenproblem()` function with reduced mass and stiffness matrices matched those outputted in the modal analysis .dat file. This led to the assumption that the respective eigenvectors, although having different dimensions and therefore obviously not being identical, must have the same information content. A closer look at the structure and content of the eigenvector from the .dat file (`EV_dat`) and the calculated eigenvector (`EV_calc`), both for the same mode, revealed a non-trivial correlation.

The length of the `EV_dat` vector is equal to the "number of nodes defined by the user" times three (information from the corresponding .dat file). So it includes the displacement of all user-defined nodes in the three dimensions (per node three entries). The `EV_calc` vector is smaller than the `EV_dat` vector and there is no direct correlation between its size and the information about the problems nodes, elements or variables provided by Abaqus. All entries of the `EV_calc` vector are contained in the `EV_dat` vector. Between large continuous sections of matching entries, there are small sections in the `EV_dat` vector that are not contained in the `EV_calc` vector. These small sections have a multiple of three entries and therefore correspond to the displacement of a single or multiple nodes. It is assumed that these entries correspond to the redundant displacements of nodes that are contact with different parts tied together in the assembly. Further research is required to investigate the exact relationships.

Based on these findings, it was opted to use a mapping matrix - `MAP` which allows to transform displacement vectors from the externally calculated "calc space" to the Abaqus - "dat space" and vise versa. The `MAP` matrix specifies the position of all `EV_calc` entries in the `EV_dat` vector. The mapping from the calc space into the dat space results in zero entries in the transformed dat-vector for the nodal displacements which are not included in the calc-vector. Since the number of these mismatched entries is small compared to the number of matched entries, the loss of information due to this transformation is not considered significant. In the QSMA routine, the mapping is applied to the specific user-defined mode that is the subject of the analysis. It has to be mentioned, that essentially equal entries in the `EV_calc` vector and the `EV_dat` vector differ slightly due to different solvers used to determine the eigensolutions and due to the applied rounding of Abaqus. Tests showed that a difference of 0.001 is sufficient to determine whether two entries are "equal" based on their absolute values subtracted from each other. A simple example of the mappings is shown in eq. (3.1). In order to increase the computational efficient and reduce the memory required for the computation, the `MAP` matrix is generated in sparse format.

$$
\underbrace{\begin{bmatrix} 1 \\ 2 \\ 3 \\ 0.1 \\ 0.2 \\ 0.3 \\ 4.0001 \\ 5.00005 \\ 6.00001 \\ 7 \\ 8 \\ 9 \\ 0 \\ 11 \\ 12 \end{bmatrix}}_{\text{EV\_dat}} \approx \underbrace{\begin{bmatrix} 1 & 0 & 0 & 0 & 0 & 0 & 0 & 0 & 0 & 0 & 0 & 0 \\ 0 & 1 & 0 & 0 & 0 & 0 & 0 & 0 & 0 & 0 & 0 & 0 \\ 0 & 0 & 1 & 0 & 0 & 0 & 0 & 0 & 0 & 0 & 0 & 0 \\ 0 & 0 & 0 & 0 & 0 & 0 & 0 & 0 & 0 & 0 & 0 & 0 \\ 0 & 0 & 0 & 0 & 0 & 0 & 0 & 0 & 0 & 0 & 0 & 0 \\ 0 & 0 & 0 & 0 & 0 & 0 & 0 & 0 & 0 & 0 & 0 & 0 \\ 0 & 0 & 0 & 1 & 0 & 0 & 0 & 0 & 0 & 0 & 0 & 0 \\ 0 & 0 & 0 & 0 & 1 & 0 & 0 & 0 & 0 & 0 & 0 & 0 \\ 0 & 0 & 0 & 0 & 0 & 1 & 0 & 0 & 0 & 0 & 0 & 0 \\ 0 & 0 & 0 & 0 & 0 & 0 & 1 & 0 & 0 & 0 & 0 & 0 \\ 0 & 0 & 0 & 0 & 0 & 0 & 0 & 1 & 0 & 0 & 0 & 0 \\ 0 & 0 & 0 & 0 & 0 & 0 & 0 & 0 & 1 & 0 & 0 & 0 \\ 0 & 0 & 0 & 0 & 0 & 0 & 0 & 0 & 0 & 0 & 0 & 0 \\ 0 & 0 & 0 & 0 & 0 & 0 & 0 & 0 & 0 & 0 & 1 & 0 \\ 0 & 0 & 0 & 0 & 0 & 0 & 0 & 0 & 0 & 0 & 0 & 1 \end{bmatrix}}_{\text{MAP}} \cdot \underbrace{\begin{bmatrix} 1 \\ 2 \\ 3 \\ 4 \\ 5 \\ 6 \\ 7 \\ 8 \\ 9 \\ 0 \\ 11 \\ 12 \end{bmatrix}}_{\text{EV\_calc}}
\tag{3.1}
$$

`external_force(MAP, M, eVec, alpha)` To calculate the force applied over the entire structure in the shape of the mode of interest, the `external_force()` function is used. The the external force vector `force` for a certain load amplitude `alpha` is computed by multiplying the calculated eigenvector `eVec` for the mode of interest with the mass matrix `M`, the transformation matrix `MAP` and the load amplitude `alpha` as shown in eq. (3.2). The transformation is necessary to map the force vector from the calc-space into the dat-space.

$$force(\alpha) = \alpha \cdot MAP \cdot M \cdot eVec \tag{3.2}$$

In addition to the external force vector, the number of nodes of the structure in the dat-space is also calculated. This is done simply by dividing the length of the force vector by three, since the force vector contains three entries per node. The number of nodes (`nodes`) is necessary for the `write_static_inp()` function.

`part_instance_nodes(filename, part_instance_name)` With this function, it is possible to obtain the `start_node` and `end_node` of a certain part instance with the name `part_instance_name` from an input file called `filename`.

`write_static_inp(modal_input_file, static_input_file, MAP, M, eVec, alpha, stabilize = False, assembly_remove = False)` The `write_static_inp()` function is used to generate an Abaqus input file called `static_input_file` which defines the analysis of the quasi-static problem for a certain load amplitude `alpha`. The `static_input_file` is in essence a modified copy of the `modal_input_file` where the bolt length is fixed after the preload step and the modal analysis step is replaced by a static step in which a calculated external force is applied on the jointed structure.

At the beginning of the new `static_input_file` a file specific "*Heading" section containing the load amplitude `alpha` is inserted. Then, a reused portion from the `modal_input_file` is appended. This part contains all the necessary information to define the structure's model such as the nodes and elements of the part instances, the material, the constraints, the interactions and so on. This portion starts with the "*Preprint" option and ends with the "*End Step" command of the `preload_step`.

After the insertion of the "reuse" part, the `static_step` is appended. At first the step header is written to the .inp file. If specified by `stabilize = True`, the stabilisation command `stabilize, allsdtol = 0.05` is added to the "*static" keyword line. This setting is an option used in this project to run the QSMA() routine on the free-free system without boundary conditions. The idea behind this is explained in detail in section 5.2.4. If the model contains boundary conditions, then the corresponding keyword and data lines are extracted from the `modal_input_file` and written into the static step after the step header. To fix the bolt length after the preload step, a specific command portion witch refers to the "Fix at Current Length" setting in the Abaqus GUI, has to be added afterwards. This procedure is necessary because of the otherwise, very large preload force which would contaminate the results (problems described in [8]). To obtain the force applied over the entire structure in the shape of the mode of interest, the `external_force()` function is called. The retrieved force vector is then written in the form *node number, degree of freedom of node, magnitude of the force* into the `static_step` after the force header was inserted. For example the data line `10, 3, 0.0028` means that at node 10 in direction of DoF 3 (z-direction) a force with the magnitude `0.0028` is applied. For the case that `assembly_remove = True` is specified, the corresponding nodes of the part instance "bolt assembly-1" are excluded from the loading. The necessary `start_node` and the `end_node` of the assembly are retrieved by calling the `part_instance_nodes()` function. The exclusion is used in the scope of this work to analysis the effect of the loading of the bolt assembly on the results (see section 5.3.6). At

the end of the `static_step` a footer section is appended which contains the commands to output the nodal displacement U in the .dat file.

`qs_response(static_job_name, eVec, M, MAP, alpha)`   The `qs_response()` function is used to retrieve the modal displacement q for a certain modal force `alpha` based on the quasi-static response of the structure. For this, the nodal displacement resulting from the Abaqus analysis of the `static_job_name` simulation, is extracted from the corresponding .dat file by calling the `u_from_dat()` function. The modal displacement q is then calculated according to the theory described in section 2.2 extended by the transformation of the obtained `u_dat` vector from the dat-space to the calc-space by utilising the `MAP` matrix as shown in eq. (3.3):

$$q(\alpha) = eVec^T \cdot M \cdot \underbrace{MAP^T \cdot u_{dat}(\alpha)}_{= \, u_{calc}(\alpha)} \tag{3.3}$$

`save_results(project_name, alpha, q)`   This function is used in order to save the obtained results of the QSMA analysis. The array data of the different load amplitudes `alpha` and the corresponding modal displacement array data q are written in two CSV files. These files are named according to the `project_name` and stored in the working directory of the project.

3.2.2   Implementation of the Evaluation Function

The so-called `evaluation()` function is implemented in the QSMA Python script, but is not part of the QSMA routine. Since Spyder does not provide a good graphical interface to display and evaluate the results of various QSMA analyses, the interactive computing environment Jupyter Notebook is used for this purpose. The `evaluation()` function must therefore be imported into such a notebook.

`evaluation(project_name, inter = False)`   The `evaluation` function is used to extract the effective natural frequencies and modal damping rations from the modal load-displacement data of a performed QSMA analysis named `project_name`. First, the QSMA data of the project is loaded and the arrays of the different load amplitudes `alpha` as well as the modal displacement q are created from the corresponding CSV files. For this it is mandatory that both files are located in the same working directory as the QSMA routine. For better understanding, it should be mentioned again that the load amplitude is equal to the modal force. Tests have shown that a load amplitude of zero results in a non-zero modal displacement. To remove this offset from the data, this displacement offset $q(\alpha = 0)$ is subtracted from all other entries in the array q. In the case where `inter = True`, the function `scipy.interpolate.splrep()` is used to fit the modal displacement as a function of load amplitude, $q = f(\alpha)$. This is done for a user-defined number of points which is set to 100 by default.

In a computational setting, it is important to consider that the results of the QSMA routine are only available in discrete form. Thus, in order to be able to calculate the forward part $\hat{f}_1$ and backward part $\hat{f}_2$ of the hysteresis curve, the modal force $f(...)$ must be equal to the discrete values of α. Therefore, $\hat{f}_1$ and $\hat{f}_2$ are not evaluated for q_i, as shown in the formulas from the theory (see section 2.2), but for "new" displacement values $q_{N1,i}$ and $q_{N2,i}$ that satisfy the constraint mentioned above. The Equations (3.4) and (3.5) show the modified

formulas which are used for the calculating of the hysteresis curve.

$$\hat{f}_1(q_{N1,i}) = 2\underbrace{f\left(\frac{q_{N1,i} + q_{max}}{2}\right)}_{= f(q_i)} - \alpha_{max} = 2\alpha_i - \alpha_{max} \tag{3.4a}$$

$$f(q_i) = f\left(\frac{q_{N1,i} + q_{max}}{2}\right) \longrightarrow q_{N1,i} = 2q_i - q_{max} \tag{3.4b}$$

$$\hat{f}_2(q_{N2,i}) = \alpha_{max} - 2\underbrace{f\left(\frac{q_{max} - q_{N2,i}}{2}\right)}_{= f(q_i)} = \alpha_{max} - 2\alpha_i \tag{3.5a}$$

$$f(q_i) = f\left(\frac{q_{max} - q_{N2,i}}{2}\right) \longrightarrow q_{N2,i} = q_{max} - 2q_i \tag{3.5b}$$

For each "modal force - modal displacement" pair, the hysteresis curve is obtained by evaluating the formulas shown above with $q_i \in [q_1, q_{max}]$ and $\alpha_i \in [\alpha_1, \alpha_{max}]$. The values q_{max} and α_{max} correspond to the currently evaluated pair. For example the construction of the hysteresis curve for the "modal force - modal displacement" pair five results in $q_{max} = q_5$ and $\alpha_{max} = \alpha_5$. The data for the forward part $q_{N1,i}$ and $\hat{f}_1$ as well as the data for the backward part $q_{N2,i}$ and $\hat{f}_2$ are stored in two separate arrays which are used for further calculations.
The instantaneous natural frequency is calculated according to the formula given in section 2.2. The implementation of this formula has been modified by a division of 2π such that the natural frequency is retrieved in Hz. To calculate the energy dissipated per cycle of vibration, the trapezoidal rule is used similar to [17] and [10]. This is done by using the `numpy.trapz()` function. Based on these results, the effective damping ratio can be calculated. The implementation for this follows the formula given in theory. The `evaluation()` function returns the arrays of `q` and `alpha` (if `inter = True`, then the new interpolated arrays) and for all "load amplitude - modal displacement" pairs the instantaneous natural frequency in the array `omega`, the energy dissipated per cycle of vibration in the array `D` and the effective damping ratio in the array `zeta`.

Chapter 4

Experimental Investigation of the Test Structure

This chapter presents the test structure, which served as the object of investigation within the scope of this work. Furthermore, the tests carried out with the physical test structure are discussed. The results from the conducted preload torque tests serve as the basis for the FE model generation. The impact hammer tests are the basis for the comparison and evaluation of the QSMA results. The respective test setup, execution and evaluation of the tests with the articulated beam structure are described below.

4.1 Brake-Reuß Beam Variant Test Structure

In research on the mechanics of jointed structures, there are a variety of different test structures with a wide range of various characteristics. In the scope of this work, the test structure was chosen based on the different variants of Brake-Reuß beams with one and three bolts already used in the research project. It was requested, that the new structure should be different from the design of the existing variants in order to have greater variability in the project. It was also requested that the design has a lap joint for the interface and that the first two bending modes be below 500 Hz to allow for reliable and easier experimental testing. Beside that, the test structures design should provoke a strong nonlinear behaviour. In addition to these specific requests, the following general requirements on a good jointed test structure design defined by Brake et al. [4] were taken into account to determine the design:

- Simple and cheap fabrication

- Usage of easy to model materials

- Simple structure that allows for a smaller/faster computational model

- Realistic interface design for applicability to a real system

Based on the mentioned requirements, a design consisting of two identical beams jointed by a single bolt and a, compared to other designs, large contact area was chosen. Aluminium EN AW 2007 was selected as material for the beams. The dimensions of the beams had to be chosen to meet the limitations of the possible machining and the material available in the workshop of the chair. Moreover because the dimensions of the beams directly influence the natural frequencies of the structure, the associated requirement on the first two bending modes had to be taken into consideration. To meet these design goals, modal analyses of the structures finite element models with different beam dimensions were conducted using Abaqus. For this, it was sufficient to use a simplified model of the test structure containing only the two beams without the bolt assembly as well as a fixed interface (tie constraint).
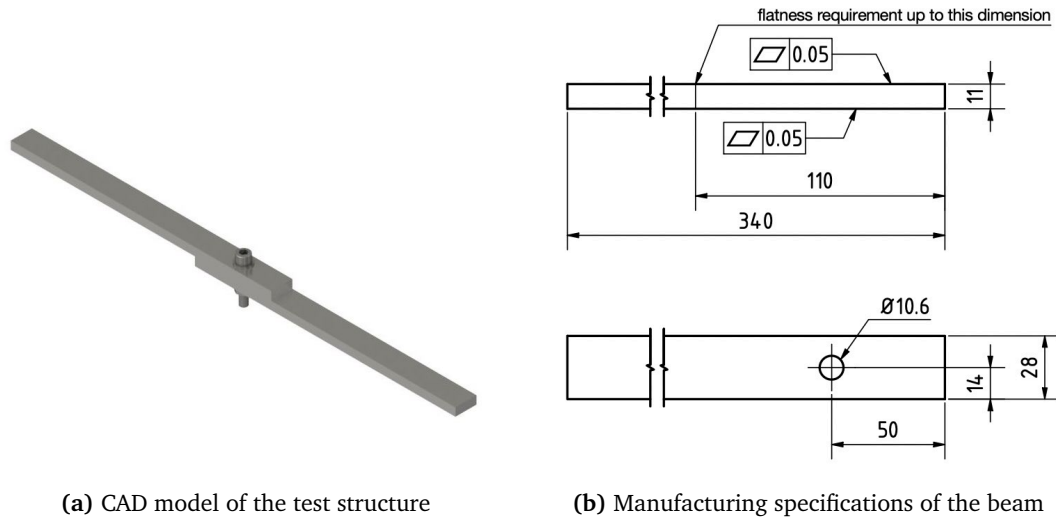
(a) CAD model of the test structure

(b) Manufacturing specifications of the beam

Figure 4.1: CAD model of the jointed beam structure and technical drawing of the beam

Through iterative testing, the final beam dimensions as shown in fig. 4.1 (b) were determined, and the beams were fabricated in the chair workshop. The beams are jointed by a bolt (DIN EN ISO 4762 M10x1,25x50), two washers (DIN 125-1 AA 10,5) and a nut (DIN EN 24034 M10). These components together are referred to as "bolt assembly" in the following. The CAD model of the assembled test structure is shown in fig. 4.1 (a). It should be mentioned that the machined aluminium beams have a slight bend along the entire length. However, due to time constraints, the parts could not be manufactured again in the scope of this semester thesis project. With regard to the experiments carried out, the two beams were jointed so that their bending caused by the manufacturing process pointed in the same direction. This was to allow the largest possible contact area at the interface and to minimise the influence of these manufacturing defects on the structures behaviour. The respective contact surfaces were marked to allow for consistency and repeatability of the tests.

4.2   Preload Torque Relationship

Bolt preload is an important parameter that has a strong influence on the behaviour of a joined structure [4]. Due to the high uncertainties involved in tightening a bolt, where the resulting preload can vary by up to $+/-35\%$ from a given torque, experiments have been conducted to investigate this relationship [12, 16]. For this purpose, a specific test procedure was applied, which is explained below.
To obtain consistent measurements, the test structure was fixed in a machining vice so that the beams were perfectly aligned and no relative movement, especially twisting, was possible due to the tightening process (see fig. 4.2 (b,c)). A piezoelectric force sensor in ring form (load washer) was positioned between the lower part of one beam and the washer and nut. The sensor was connected to the interface of the measurement computer via a charge amplifier. As shown in fig. 4.2 (a), a digital torque wrench and a normal wrench for counter-holding the nut were used to apply the preload. The wrench was counter-held on a steel cylinder attached to the lab table to avoid twisting of the entire bolt assembly without tightening and to ensure an accurate torque application. For the data acquisition, hardware and software of the Siemens LMS-System were used. Parameters for both the charge amplifier as well as LMS were set to the specifications of the load sensor.
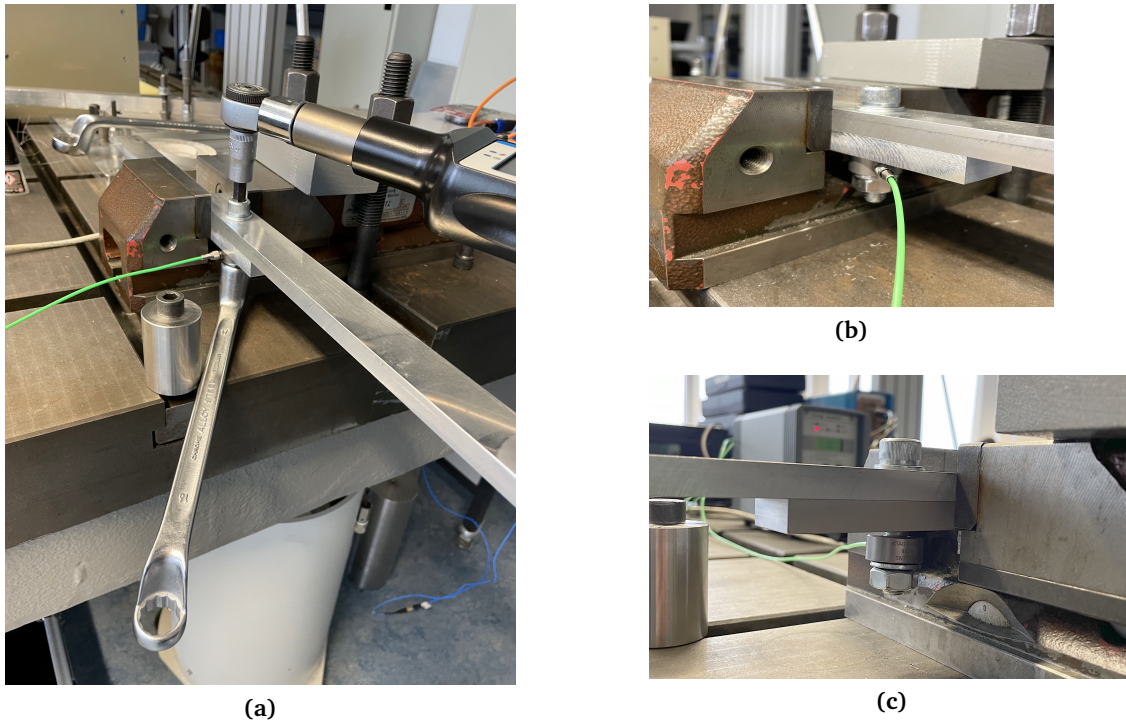
(a)

(b)

(c)

Figure 4.2: Experimental setup of the preload torque measurements

In order to capture changes due to the number of load cycles, a measurement series of 12 runs was conducted. Before the start of all measurements, the charge amplifier was reset when the sensor was unloaded. For one measurement run the torque was increased from the unloaded state to a maximum load of 50 Nm in 5 Nm steps. After the measurement was manually started, the torque was increased rapidly in about 1 to 2 seconds from one torque level to the next one. In between it was released for about 4 seconds in order to measure the constant preload in the bolt for each torque level. It was tried to keep the derivation from the actual and the expected torque level around $+/-1$ Nm. After each measurement run, the bolt was loosened so that the force sensor was completely unloaded.

To obtain the relationship between preload and torque for each test run from the corresponding time plot in staircase shape, the force in the sections of the measurement with constant preload was averaged for each torque level. The resulting torque-preload-curves can be interpreted as linear and are plotted in fig. 4.3 for all runs. The curves of the first six runs show a significant drop in the slopes as the number of conducted runs increases. Comparing the slopes of run 7 to 12, the curves do not differ as significant as the first ones and they seem to converge to a certain slope. It is assumed, that the multiple loading of the structure leads to an altering effect up to a certain degree which influences the contact conditions and thus the slopes of the curves. One indicator of this is the visible wear on the contact regions of the washers on the beams. It is important to mention that the exact effects of the occurring friction are highly complex due to various multi-physics and multi-scale aspects which are not simple to describe [5]. The obtained results match the ones of previous conducted experiments in the research project. The relationship between torque and preload can be estimated by a linear curve fitting of the last six curves as displayed in fig. 4.3. By doing so one can obtain the simplified linear preload - torque relationship for the test structure:

$$F_M = k_{avg} \cdot T_A = 237,91 \cdot T_A \tag{4.1}$$

To check the feasibility of the experimental results, an analytical relationship, also used by Wang et al. [17] in their studies, was used to verify the results. The relation between
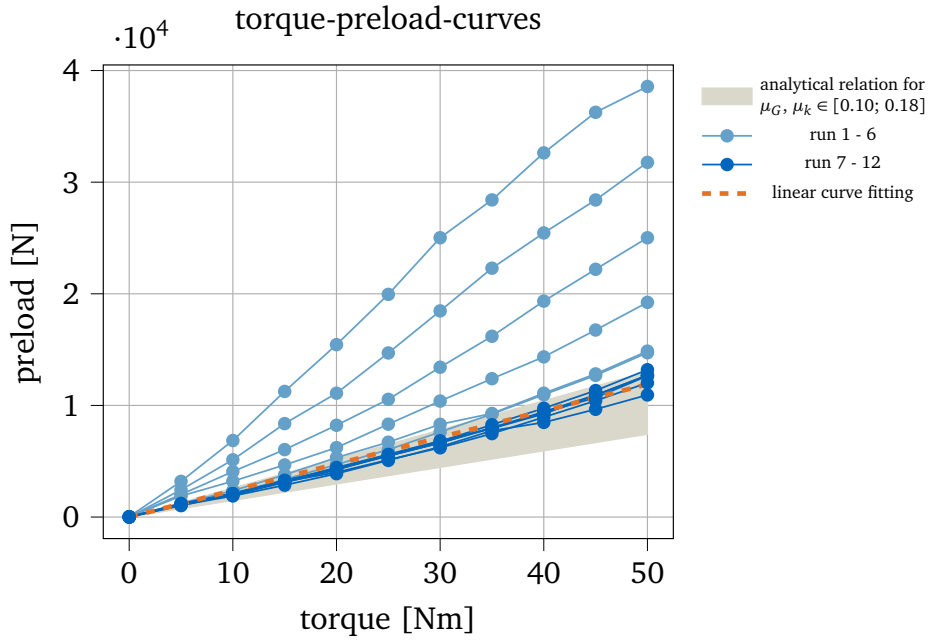
Figure 4.3: Resulting relationship between torque and preload. Linear curve fitting of the last six experimental slopes and analytical relation.

F_M and T_A from [9] is depended on certain geometrical parameters of the bolt and can be expressed by eq. (4.2). The parameters are listed in the corresponding Jupyter notebook of the evaluation.

$$F_M = T_A \cdot \left(\frac{P_h}{2\pi} + \mu_G \cdot \frac{d_2}{2cos(\frac{\alpha}{2})} + \mu_k \cdot \frac{d_w + d_a}{4} \right)^{-1} \tag{4.2}$$

Under the simplified assumption that the friction coefficient in the thread is equal to the friction coefficient in the head contact region ($\mu_G = \mu_k$) the analytical relation was evaluated for a coefficient range of 0.10 to 0.18 and plotted in fig. 4.3. The friction coefficient range was taken from [13] according to the bolt and nut specifications of the assembly. The results show, that the fitted slope of the experimental data is in the range of the analytical slopes which indicates meaningful results.

4.3 Impact Hammer Test Procedure

Impact Hammer tests were performed on the test structure to investigate its nonlinear behaviour and to obtain backbone curves to serve as the basis of comparison for the QSMA routine.
With the intention to approximate free boundary conditions as good as possible, the test structure was suspended from an experimental rig by two thin polyamid strings (see fig. 4.4 (b)). This attachment method is, in contrast to a clamped boundary condition setup, commonly used in shaker or impact hammer experiments in order to minimise the energy dissipation due to the attachment to another structure [4]. The test structure was positioned in such a way that the attachment points of the strings were located at nodal points of the examined first two bending modes (see fig. 4.4 (a)). The nodal points were obtained by a modal analysis of the system conducted with Abaqus. The lengths of the polyamid strings were adjusted so that the structure was leveled. One accelorometer was super glued to the top of one beam
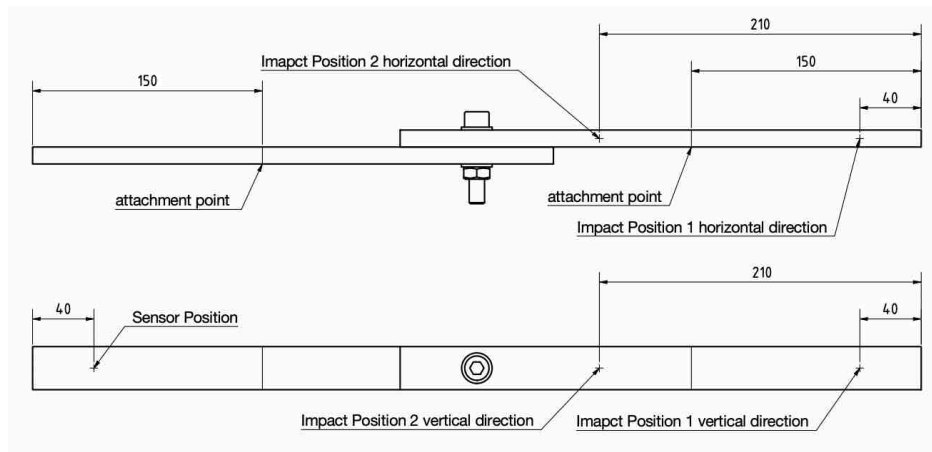
(a)
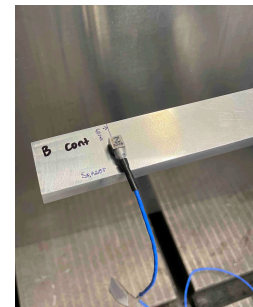
(b)   **(c)**

Figure 4.4: Experimental setup of the jointed beam structure for the impact hammer tests

and not removed for all conduced tests (see fig. 4.4 (c)) . The sensor as well as the impact hammer were connected to the Siemens LMS-System interface and the associated software was used for the data recording. The carried out experiments were intended to asses the influence of different torque levels, different impact positions and different impact forces on the damping ratio as well as on the natural frequencies of the structures first two bending modes. In addition to that, the measurement-to-measurement repeatability was investigated based on the results of two measurement runs.

For the first run, the structure was tested with the torque levels of 3, 5, 8, 10, 20, 35 and 50 Nm, as shown in fig. 4.5. Per torque level a total of eight different impact tests were performed, except for the 3 Nm torque level where only the low impact force level was tested. The second measurement run consisted only of tests for the impact position 2 and the torque levels 3, 5, 10, 50 Nm with an otherwise unchanged test procedure.

The impact direction was chosen so that either the first bending mode in horizontal ($+X$) or in vertical ($-Z$) direction was targeted by the excitation. The different impact positions are shown in in fig. 4.4 (a). The impact forces were selected according to the impact directions. For each direction the structure was excited by a low ($60N$ or $80N$) and a high ($400N$ or $600N$) force level. It was taken care, that the detected force by the load cell in the impact hammer tip were in the range of $+/-20\%$ of the targeted impact force level (measurement error of the setup) and no double impact occurred. Throughout one measurement run, the torque was increased without loosening the bolt assembly in between. The same setup and procedure as for the torque-preload measurements was used to tighten the bolt. The accelerometer was not removed for either measurement run. Before each impact test, the position of the polyamid springs was readjusted to the correct position and it was made sure that the structure was not swinging. The second measurement run was conducted after
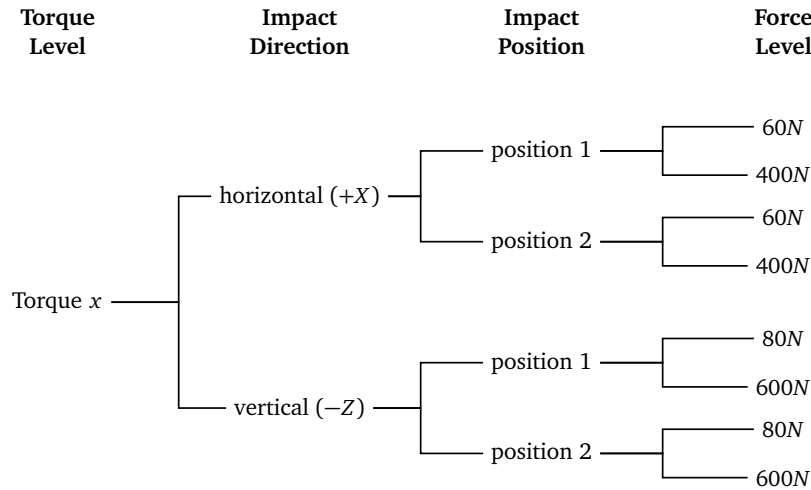
Torque Level	Impact Direction	Impact Position	Force Level

Figure 4.5: Schematic test procedure of the impact hammer experiments

the beams were completely separated for one night (approx. 18h).

An existing Matlab routine was used to analyse the experimental data. The routine was slightly modified in order to retrieve the damping ratio and natural frequency over the amplitude in $[mm]$ instead of $[m/s^2]$. This is advantageous for a later comparison of the experimentally obtained backbone curves with the results from the QSMA simulations. Therefore, the acceleration data is filtered (high-pass filter) and then integrated with the `cumptrapz()` function to obtain the velocity data. This procedure is then repeated to obtain the displacement data. After integration and filtering, the analytical signal is obtained by a combined modal filtering and Hilbert transform. The results of a polynomial fit of the amplitude and phase are then used to obtain the backbone curves. The cutoff frequency of the used Butterworth filter, the time interval as well as the polynomial order of the applied fitting had to be manually adjusted to obtain useful results. Python and Matplotlib were used to visualize the results.

A large amount of data was obtained through the experiments carried out. With regard to the focus of this work, a detailed and extensive evaluation of the experimental results is omitted. In the course of this, four representative data plots of experiments with horizontal $(+X)$ impact direction are used in the following to evaluate whether the design goal of nonlinear behaviour of the test structure was achieved. In doing so, the obtained backbone curves will be briefly explained and the results interpreted. It should be mentioned that the results of the experiments with vertical $(-Z)$ impact direction are not discussed here. This is because these data were not used to evaluate the QSMA routine in the context of this work. The reason for this is given in chapter 5. The corresponding backbone curves can be used for further investigations and are provided in the data directory of this thesis.

The obtained natural frequency and damping ratio curves of the experiments from the measurement run 1 with the impact position 1, the horizontal $(+X)$ impact direction, a force level of 60 N assessed for the torque levels 3, 5, 8, 10, 20, 35 and 50 Nm, are shown in fig. 4.6. Looking at the natural frequency curves, there is no obvious correlation between the torque level and the resulting frequency, as one would expect with linear behaviour (e.g. higher preload leads to higher frequencies). This indicates the non-linear behaviour of the test structure. It is important to note that an unexpected softening of the test structure for the torque levels 35 Nm and 50 Nm can be observed when considering the natural frequency curves obtained. To rule out an error in the evaluation, these results were compared with

those from the experiments with a higher force level of 400 N and with those from measurement run 2. In addition, the corresponding FRFs were checked. It was found that these unusual results could be confirmed. Based on these findings, it is assumed that this softening is due to geometric changes of the contact surfaces of the beams due to the tightening process. However, to investigate this in more detail and to further confirm the obtained results, a comparison with results from a larger series of experiments is necessary.
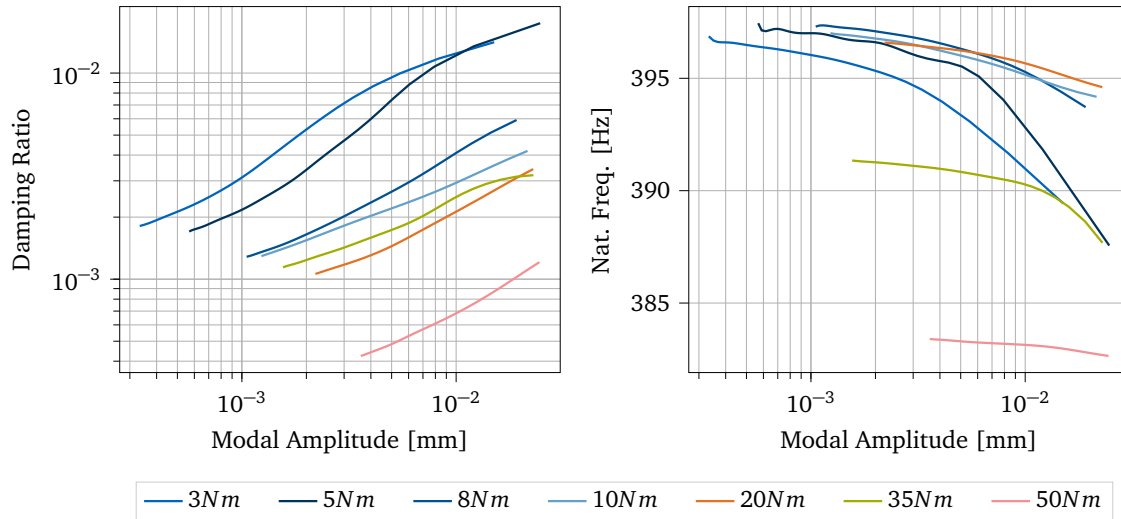
Figure 4.6: Natural Frequency change and Damping Ratio assessed for the Torque Levels 3, 5, 8, 10, 20, 35 and 50 Nm all with: measurement run 1, Impact Direction = horizontal $(+X)$, Impact Position = position 1, Force Level = 60 N

The plots in fig. 4.7 show the natural frequency and damping ratio curves of the conducted tests from the measurement run 1 with a torque level of 10 Nm, the horizontal $(+X)$ impact direction and a force level of 400 N for the two impact positions 1 and 2. Beside the slight difference in the resulting damping ratio curves, a clear influence of the impact position on the natural frequency can be seen. It should be noted that this difference is less pronounced in the other comparisons not listed here, but the influence of the position can still be seen.
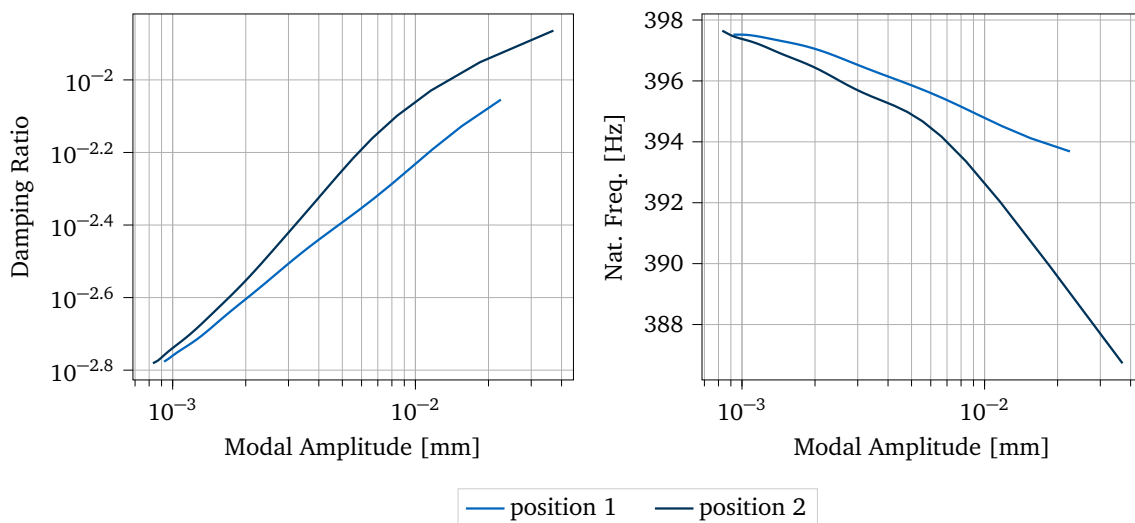

Figure 4.7: Natural Frequency change and Damping Ratio assessed for the Impact Positions position 1 and position 2 both with: measurement run 1, Torque Level = 10 Nm, Impact Direction = horizontal $(+X)$, Force Level = 400 N
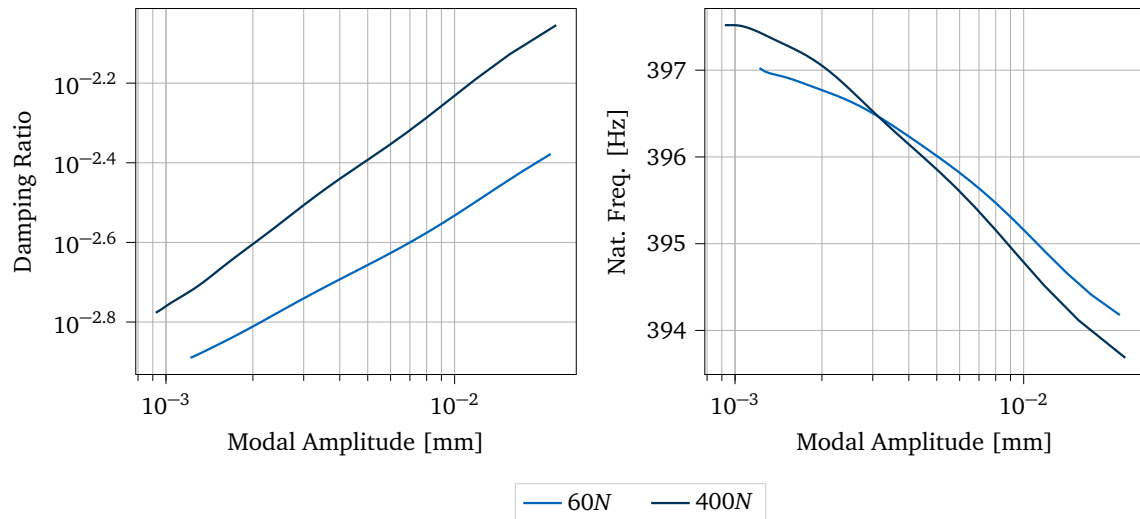
Figure 4.8: Natural Frequency Change and Damping Ratio assessed for the Force Levels of 60 N and 400 N both with: measurement run 1, Torque Level = 10 Nm, Impact Direction = horizontal ($+X$), Impact Position = position 1

The natural frequency and damping ratio curves of the experiments from the measurement run 1 with a torque level of 10 Nm, the impact position 1, the horizontal ($+X$) impact direction assessed for the force levels of 60 N and 400 N are shown in fig. 4.8. The results obtained show that the impact force also influences the response of the joined structure, which can be seen in the different natural frequency curves.

The plots in fig. 4.9 show the natural frequency and damping ratio curves of the experiments from measurement run 1 and run 2. Both runs were conducted with a torque level of 10 Nm, the horizontal ($+X$) impact direction, the impact position 2 and a force level of 60 N. The natural frequency as well as the damping ratio curves of the two measurement runs show clear differences. This nonlinear behaviour complies with the findings of Smith et al. [14] that jointed structures show little repeatability in their response.

In summary, it was found that natural frequency and the damping ratio of the test structure depend on the impact position, the impact amplitude and the torque level. The structures response can change as a function of controllable variables, such as the bolt preload, and unknown variables which is observed by the lack of repeatability [14]. It is difficult to comprehensively determine the nonlinear behaviour of the jointed beam structure due to various influencing factors (e.g. surface finish, alignment, asperity distribution, residual stresses, machining variations, curvature, etc.) [14]. The results show that the test structure has a clear non-linear behaviour, which makes it suitable for the analysis of its FE model with QSMA.
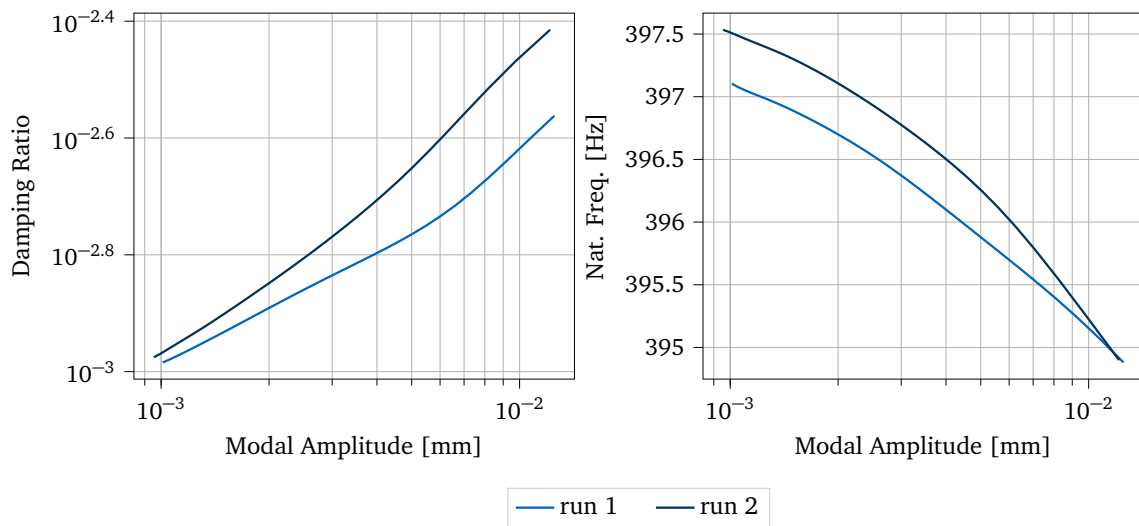
Figure 4.9: Natural Frequency Change and Damping Ratio assessed for measurement run 1 and run 2, both with: Torque Level = 10 Nm, Impact Direction = horizontal $(+X)$, Impact Position = position 2, Force Level = $60N$

Chapter 5

QSMA Routine Testing and Parameter Influence

In the following section, the implemented QSMA routine is tested by applying it to a high fidelity finite element model of the test structure described in 4.1. The results obtained are evaluated with the use of the experimental data and the effects of certain simulation settings and model parameters are investigated.

First, the creation of the finite element model of the test structure is described. The following section then deals with the investigation of the structure in a free-free configuration. In the course of this, the problems arising from the absence of boundary conditions are addressed and different approaches to solving this problem are investigated. In this configuration, the first bending mode of the structure in the horizontal direction was chosen as the subject of the investigations. In the next section, the effect of certain model parameters and routine settings on the QSMA results of the structure with additional boundary conditions (one beam fixed on one side) are evaluated. For this configuration, the second bending mode of the structure in the horizontal direction was chosen as the object of the study. As mentioned, for both configurations, the modes in the horizontal direction were chosen as the object of study. This is due to the fact that the agreement between the experimental results and those of the QSMA routine, both for the free-free and for the system with boundary conditions, is significantly greater for the modes in horizontal direction than for the modes in the vertical direction.
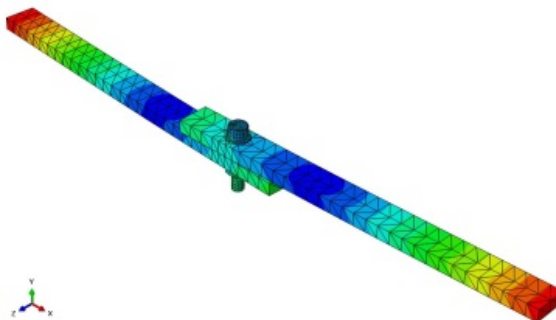

Figure 5.1: First bending mode in horizontal direction of the test structure in free-free configuration

5.1 FE Model Creation of the Test Structure

The finite element model of the test structure was created using the Abaqus CAE 2020 GUI. In order to ensure the functionality of the routine, the requirements listed in chapter 3.1 were

taken into account when creating the model.

The assembly consists of two beam part instances and one bolt assembly. The individual components of the bolt assembly (bolt, nut and washers) were exported from a CAD component library for standard parts and combined into a single continuous part, which is used to joint the beams. A material with a mass density of 2.85E-09 ton/mm^3, a Young's modulus of 72500 MPa and a Poisson's ratio of 0.327 was defined and assigned to the beam parts (aluminium EN AW 2007). For the bolt assembly, a material with a mass density of 7.85E-09 ton/mm^3, a Young's modulus of 211000 MPa and a Poisson's ratio of 0.330 (steel grade 10.9) was defined. The material parameters of both materials were not changed in the course of the simulations carried out within the scope of this work.

The contact at the interface of the jointed beams is defined as an interaction in Abaqus. The implementation of this specific contact formulation was taken from an existing FE model which is also subject of investigations within the research project. Since a detailed explanation of the underlying theory behind the development of the contact formulation used would go beyond the scope of this work, the following only refers to the practical implementation of this interaction in Abaqus. For a more in-depth treatment of the theory, reference is made to the corresponding work in the research project which is not yet fully published. For the interaction, the contact pair algorithm, the surface-to-surface discretization method and the finite sliding formulation are used as general settings. If not explicitly marked, the following settings and parameters were not changed in the course of the investigations. The interaction behaviour of the contact in tangential direction is specified by the following setting:

- Friction formulation: Penalty

- Friction coefficient: Changed in the course of the investigations

- Shear stress: No limit

- Fraction of characteristic surface dimension (Elastic slip): 0.005

The corresponding behaviour in normal direction is specified as follows:

- Pressure-Overclosure: Linear

- Constraint enforcement method: Default (direct)

- Contact stiffness: 1E+07

The bolt assembly is attached to the jointed beams with a tie constraint between the bolt head washer and one beam and another tie constraint between the nut washer and the other beam. Partitions were added to the parts to ensure less distorted elements during meshing and to allow the use of different mesh densities for a part. This serves in particular for better mesh refinement in the area of the interfaces of the beams. The beam parts as well as the complete bolt assembly are meshed with tetrahedral elements (C3D10 A 10-node quadratic tetrahedron). The Abaqus default algorithm for Tet-shaped elements was used as the mesh control (Technique: Free, Algorithm: use default algorithm). In the course of the investigations only the seed position (uniform or bias seeding) and the corresponding mesh density were changed.

After the initial step, which is created by Abaqus as default, two analysis steps were defined - a preload step (Static, General) followed by a model analysis step (Frequency). The preload step is specified by certain non-default settings which are listed below:
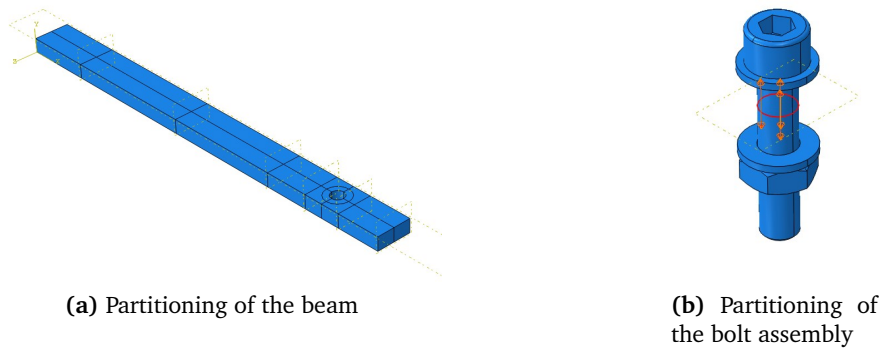
- Time period: 1

- Nlgeom: On

(a) Partitioning of the beam

(b) Partitioning of the bolt assembly

Figure 5.2: Partitioning of the beam and the bolt assembly. The latter shows the applied bolt load on the symmetry partition plane of the bolt assembly.

- Incrementation Type: Automatic

- Maximum number of increments: 100

- Increment size: 1 (Initial), 1E-05 (Minimum), 1 (Maximum)

In the preload step a load of the Type "Bolt load" is applied to the symmetry partition plane of the bolt assembly as shown in fig. 5.2. The load is further specified with the settings Bolt axis: Surface normal, Method: Apply force and the Amplitude: (Ramp). The Magnitude of the preload force is the only parameter which was changed during the examinations. The non-default settings of the modal analysis step are set as follows:

- Nlgeom: On

- Eigensolver: Lanczos

- Number of eigenvalues requested: Value: 10

5.2 Free-Free System

Applying the QSMA routine to the free-free model of the test structure without any boundary conditions would correspond to the experimental suspended configuration. This setup, however, leads to unusable results as shown in fig. 5.3. This is because the quasi-static problem eq. (2.4) becomes singular due to the rigid body modes [10].
Lacayo et al. [10] have solved this problem by modifying the quasi static problem to eliminate that rigid body motion. This is done by constraining the quasi static response as being (M-) orthogonal to the rigid body motion of the system. For this purpose, a certain transformation of the EOM is applied. However, this approach cannot be applied to the QSMA routine presented here. This is because Abaqus does not provide the necessary interface to access and modify the EOM. Consequently, another method or a certain simulation setting had to be found so that the influence of the rigid body modes on the QSMA results of the free-free system can be eliminated. For this purpose, different approaches to solve this problem are presented in the following and their effectiveness is evaluated based on experimental data. All QSMA analyses in this section were performed with a bolt preload of 2249N, which corresponds to the experimental tests of the structure with a torque of 10 Nm.
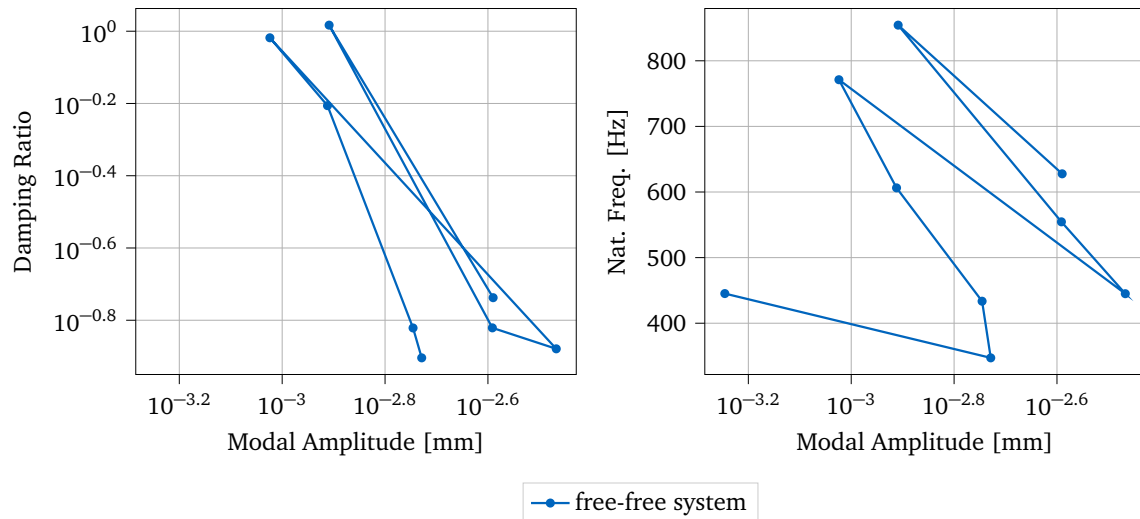
Figure 5.3: QSMA analysis of the coarse mesh model in complete free-free configuration with `alpha = np.linspace(0,40000,10)`, $\mu = 1.1$ and a bolt preload = 2249 N

5.2.1 Experimental Data and Material Damping

In order to compare the damping ratio curves obtained with the QSMA routine with the corresponding experimental data, the absence of material and other forms of linear damping in the FE model must be taken into account. Since the damping of the test structure is only analysed for a single mode, the material damping is not amplitude-dependent and thus a constant value that must be subtracted from the experimental data [16]. Following the approach of Wall et al. [16], the experimental data was subtracted with different constant values for the material damping. This covers a certain range of curves that can be compared with the results of the QSMA routine. The choice of this interval should be consistent with a certain power law relationship of the damping [2]. Since an exact value of the linear damping for the test structure cannot be determined and the experimental data differ greatly from the simulation data, the interval of the subtracted values was greatly increased (compared to the interval used in [16]) in order to find a correlation between the data.

It was found that the results of the experimental test runs with a torque of 10Nm and a horizontal (+X) impact direction differed much less from each other than from all the obtained QSMA results of the free-free system. For this reason, and because the results are only compared quantitatively, it was decided to compare the simulation results with the experimental results of a single representative test run (impact position 1, run 1, torque level = 10 Nm, impact direction = horizontal (+X), force level = 400N). This allows a better overview for the comparison of the recorded curves.

5.2.2 Inertia Relief

To solve the problem of the influence of the rigid body modes on the QMSA results, Wall et al. [16] opted to use inertia relief in their analysis. In the preload step, an interia relief load as well as an additional rotational constraint were applied. In the quasi static loading step, only interia relief, without an additional constraint, was applied. These settings allowed them to balance the externally applied forces on the tested free-free model [16].

However, the attempt to use inertia relief in the mentioned configuration did not lead to success. Different variations of the inertia relief setup were tested and it was not possible

in any tests to obtain converging results without adding at least one additional boundary condition to the system in the static analysis step.

These results are consistent with the Abaqus documentation, which states that inertia relief is not supported for models consisting of unconnected regions, even if a contact is defined between them (except for the tie constraint). Thus, the use of inertial relief for such models may result in poor or no convergence [7].

5.2.3 Spring Configuration Method

Another approach to constrain the rigid body motion is to use springs attached to the test structure and connected to the ground. This should theoretically lead to converging results without changing the systems properties as much as real boundary conditions do and without introducing additional damping that could contaminate the results.

This concept was tested by evaluating the QSMA results of the jointed beam model for various spring configurations. These configurations differ from each other in the number of spring assemblies and their mounting position, as well as in the stiffness of the springs within the configuration. One spring assembly consists of three separate springs, all attached to the structure at the same connection point, but having different orientations and thus attachment points to the ground. One spring is oriented in the x-direction, one in the y-direction and one in the z-direction. The corresponding connection point of the springs to the structure within an assembly is visualized by Abaqus with an orange sphere, as shown in fig. 5.4. Within a spring configuration, all springs were assigned the same stiffness. Both the number of springs
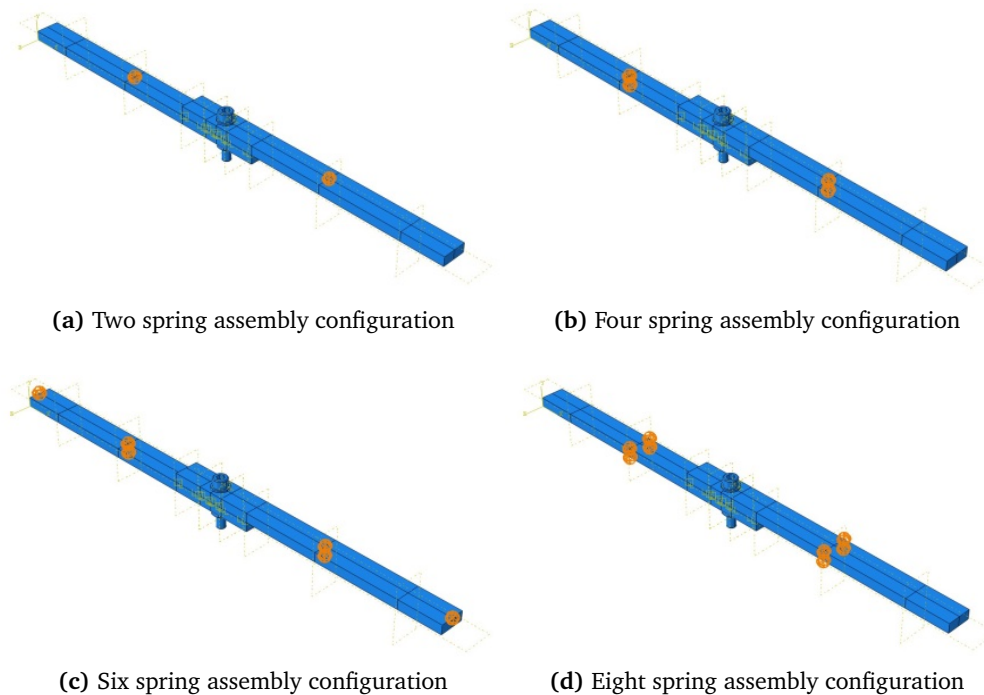

(a) Two spring assembly configuration

(b) Four spring assembly configuration

(c) Six spring assembly configuration

(d) Eight spring assembly configuration

Figure 5.4: Spring assembly attachment positions of the different configurations. Each spring assembly consists of three springs attached to the same point on the structure (orange sphere) each with a different orientation (x,y,z) and thus attachment point to the ground.

and the attachment position of the spring assemblies were found to have a direct influence on the convergence of the results. For example, Abaqus aborted all QSMA analyses of the model in spring configuration fig. 5.4 (a), where the structure is connected to the ground

with two spring assemblies (see fig. 5.5). Even comparatively high spring stiffness values did not lead to convergence. In contrast, both configuration fig. 5.4 (b) with four spring assemblies and configuration fig. 5.4 (c) with six spring assemblies attached to the jointed beams led to converging results. The QSMA analyses of these configurations were performed using the coarse mesh model of the structure (see section 5.3.1) and the different spring stiffness values 0.5553, 1, 5, and 10. It was found that the results in all configurations converged only for the highest spring stiffness value of 10. The results are plotted in fig. 5.5.

The investigations carried out have thus shown that in addition to the number and position of the spring assemblies, the spring stiffness significantly determines the convergence of the results. In the course of the investigations, the analysis of the fine mesh model (see section 5.3.1) in a configuration with eight spring assemblies (fig. 5.4 (d)) gave the best results. The results obtained for this configuration most closely match the shape of the experimental damping ratio curve for a material damping of 4e-5 (see fig. 5.5). Nevertheless, there is still a large offset in the form of a shift along the y-axis. The corresponding natural frequency curves differ greatly due to a different slope as well as a very different maximum natural frequency.
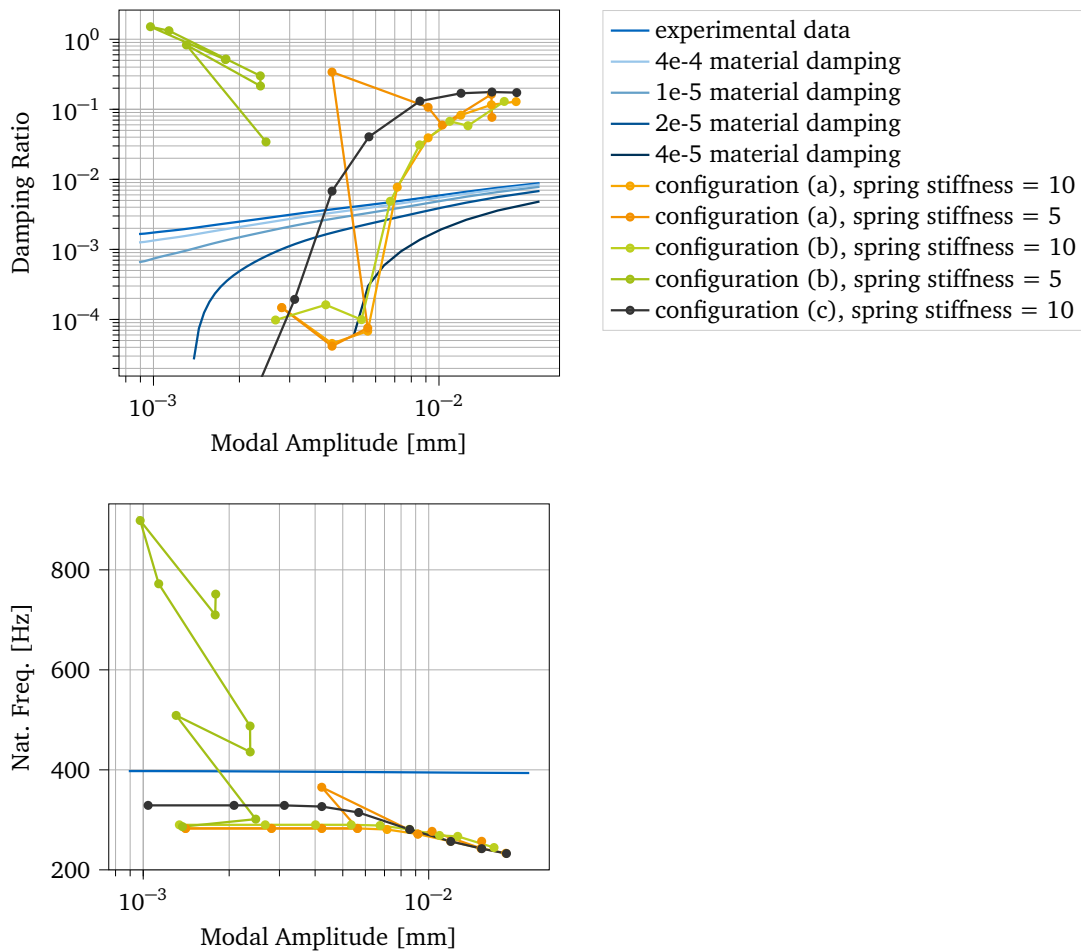

Figure 5.5: QSMA results of the Spring Configuration Mechanism test - All QSMA analyses were conduced with `alpha = np.linspace(0,40000,10)`, preload = 2249 N and μ = 1.1. Configurations with a spring stiffness of 5 as an example of non-converging results.

5.2.4 Stabilization Mechanism

Abaqus provides a mechanism to stabilize unstable quasi-static problems trough the automatic addition of volume-proportional damping to the model [15]. The use of this mechanism thus presents itself to constraining the rigid-body motion of the system for the QSMA use case [3, 8]. The general applicability and effectiveness of this particular stabilization technique, when applied to the QSMA analysis, is examined below.

As described in section 3.1, the QSMA routine was programmed such that this stabilization mechanism can be applied to the analysed model. Various tests were carried out to evaluate the effectiveness of this mechanism in removing the rigid body modes and the resulting unwanted influence of the additional damping on the results.

All initial QSMA analyses were performed with the fine mesh model and the default stabilization mechanism activated in the preload and quasi static steps. Using the mechanism in its default configuration results in an adaptive automatic stabilization with the stabilization energy tolerance ALLSDTOL = 0.05. The corresponding input file command is: `*STATIC, STABILIZE`. The tests of the jointed beam structure were carried out with different friction coefficients and preload values. The resulting damping ratio and natural frequency curves
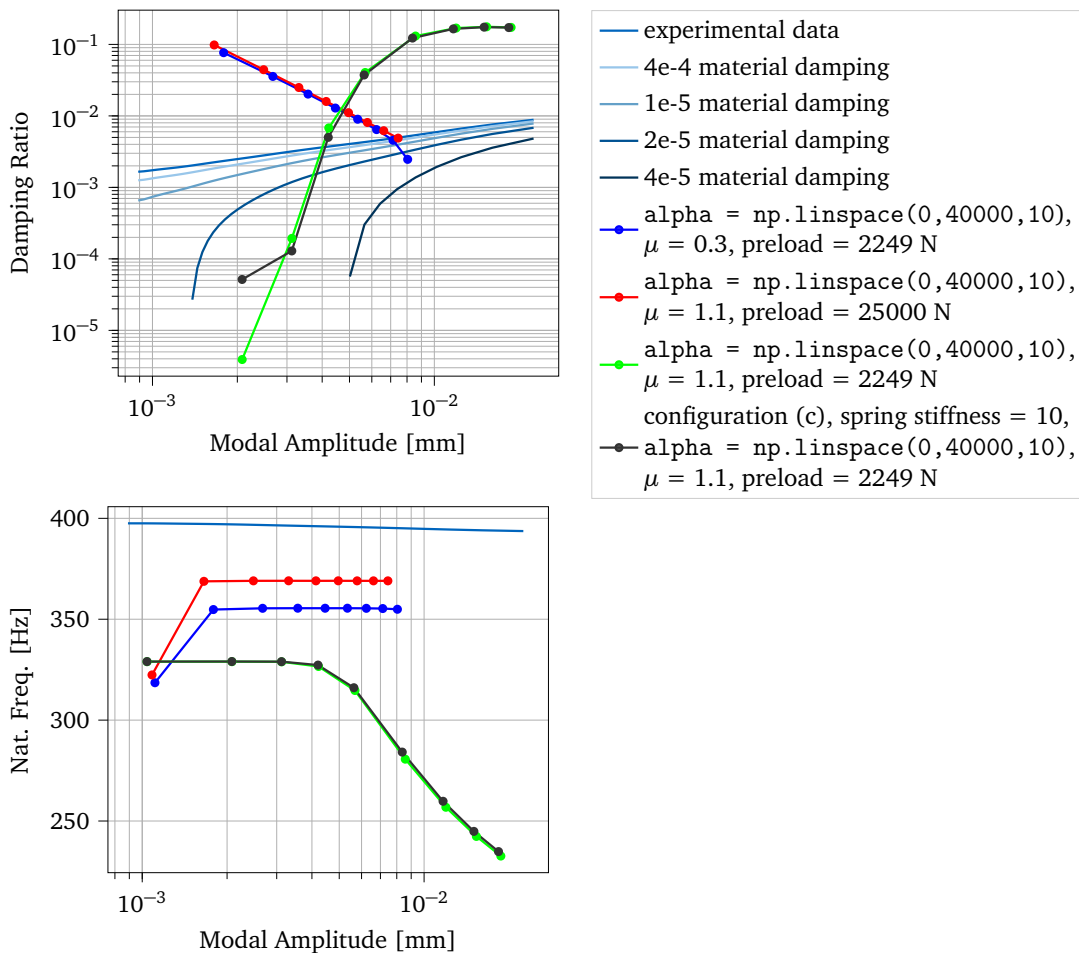

Figure 5.6: QSMA results of the different Stabilization Mechanism tests

show that the preload and the friction coefficient have a strong effect on the QSMA results and the effectiveness of the stabilization mechanism. The influence of these parameters is evaluated separately in section 5.3. The most important finding is that the results of the stabilization test with `alpha = np.linspace(0,40000,10)`, $\mu = 1,1$ and preload = 2249

N show a high agreement with the promising results of the analysis with spring assemblies in configuration (c) and a spring stiffness of 10. In a direct comparison between the stabilization mechanism and the spring configuration method, it can be said that the latter leads to a comparably higher implementation effort and uncertainty due to configuration dependency. For this reason, it was decided to investigate the stabilization mechanism further and to use it in order to validate the QSMA routine.

5.2.5   Stabilization Mechanism - Validation of the QSMA Routine

Due to the large differences between the QSMA results presented and the experimental data, the question arises whether the routine can provide reliable results at all. To answer this question and thus validate the functionality of the QSMA routine, special tests were conducted with a modified version of the free-free model of the test structure.
The FE model of the jointed beam structure in the free-free configuration has been modified by replacing the contact (interaction) at the interface of the beams with a tie constraint. This modification removes all sources of non-linearity within the model. If the QSMA routine is working properly, the results of the analysis with this model should agree with the linear behaviour of the structure. More specifically, the natural frequencies obtained should match those obtained from the modal analysis step of the structure.
The QSMA analyses of this FE model were performed with the stabilization mechanism in different configurations. In this way, the effect of the different mechanism settings on the QSMA results was evaluated. All test were conducted with the modified coarse mesh model, `alpha = np.linspace(0,40000,100)`, $\mu = 1.1$ and a bolt preload of 2249 N.

The implementation of the stabilization mechanism with a constant damping factor applied over the duration of the step with the default stabilization energy tolerance ALLSDTOL = 0.05 (`*STATIC, STABILIZE, FACTOR = damping factor, ALLSDTOL`) resulted in jittering in the obtained QSMA results. As a result, this approach was not investigated further.
The stabilisation mechanism with adaptive automatic stabilization changes the damping factor over time and showed significantly better results. This mechanism was tested both with the standard stabilization energy tolerance ALLSDTOL = 0.05 (`*STATIC, STABILIZE`) and with non-standard stabilization energy tolerances (`*STATIC, STABILIZE, ALLSDTOL = accuracy tolerance`) ranging from 0.02 to 0.04.
As recommended by Abaqus, the damping factor was not increased above the default value of ALLSDTOL = 0.05 due to the otherwise high influence of the mechanism on the actual damping of the system [15]. The analyses were performed with ALLSDTOL = 0.02, 0.03, 0.04, 0.05 and 0.05 with nlgeom = NO. It was found that for ALLSDTOL = 0.02 the calculated damping factor is too small to control the instability of the system. Therefore, the results are not plotted in fig. 5.7. It could be shown that the analysis setting nlgeom = NO or nlgeom = YES (default) has no influence on the results. The curves match exactly, which is why the resulting curves of ALLSDTOL = 0.05, nlgeom = NO cannot be seen in the plot, as they are below those of ALLSDTOL = 0.05.
The resulting curves of the damping ratio differ only slightly for the different stabilisation settings. As the modal amplitude increases, the damping ratio decreases sharply. Since the modified FE model does not contain any damping sources, in theory no damping should be detected. Thus, the resulting damping comes from the stabilisation mechanism.
The resulting frequency curves show for all test cases that the natural frequency decreases with increasing modal amplitude and that the slopes converge to a certain constant frequency value. The lower the value of ALLSDTOL, the lower this natural frequency. If one compares the resulting constant natural frequency with the frequency of the mode under investigation
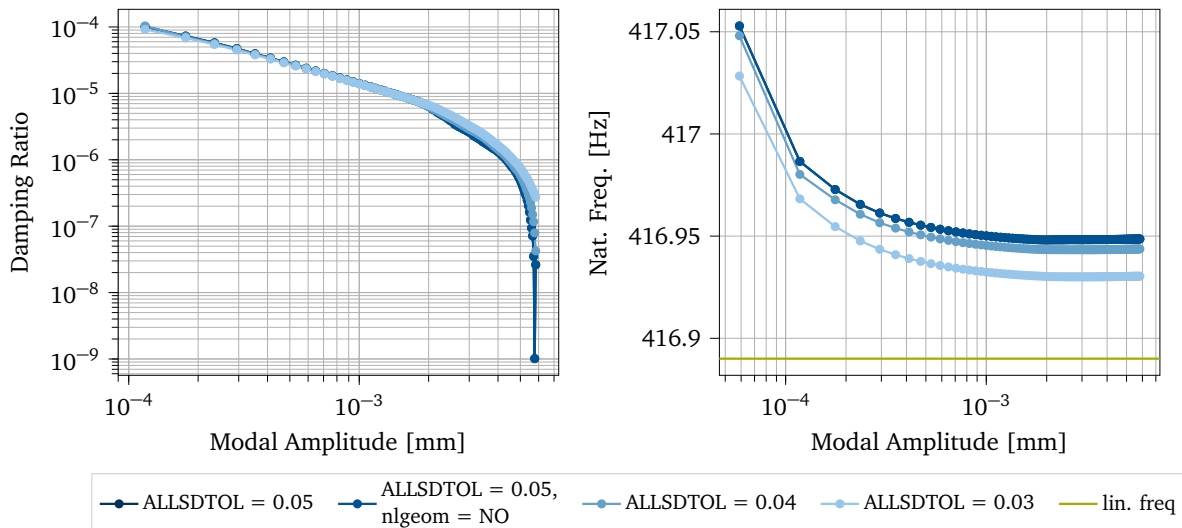
Figure 5.7: QSMA results - Validation of the QSMA Routine

determined from the modal analysis (416.89 Hz), only a small difference can be observed. ALLSDTOL = 0.05 (both configurations) resulted in a constant natural frequency of 416.95 Hz, ALLSDTOL = 0.04 in a constant natural frequency of 416.94 Hz and ALLSDTOL = 0.03 in a constant natural frequency of 416.93 Hz.

Based on the results obtained, the function of the QSMA routine could be validated. In general, it can be said that the damping caused by the stabilisation mechanism affects the QSMA results. Although the results for this particular test case are promising, further research is needed to assess whether this mechanism can be used to stabilize the actual system without distorting the results. Jewell et al. [8] concluded that adaptive stabilization should not be used (ALLSDTOL = 0) because it appears to lead to unwanted dissipation in their studies. Based on this, they performed their further analyses with a constant damping factor within the stabilization mechanism.

5.3 System with Boundary Conditions

The boundary condition model is a modified version of the free-free model of the test structure with one end of a beam fixed. This was implemented by applying a boundary condition at the region shown in fig. 5.8 which was defined as Encastre (U1 = U2 = U3 = UR1 = UR2 = UR3 = 0). This model allows to evaluate the impact of certain FE model parameters and QSMA routine settings on the analysis results by eliminating the problems related to the singularity of the free-free test model. One drawback is that the QSMA results of the boundary condition model can only be evaluated qualitatively. This is due to the fact that the experimental testing of the structure attached to a fixture would not allow to distinguish between the non-linear effect originating from the bolt or the fixture.

The test procedure shown below can be similarly performed with the system in free-free configuration using one of the promising stabilization mechanisms mentioned above. However, their applicability needs to be further investigated and confirmed.
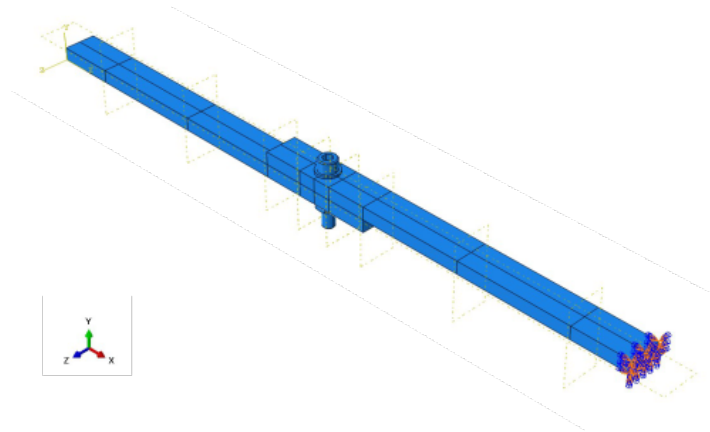
Figure 5.8: FE model of the test structure with applied boundary conditions

5.3.1 Influence of the Mesh

The mesh and the corresponding resolution of the FE model have a strong influence on the results of the QSMA routine. This is due to the fact that a certain resolution, especially in the interface region of the beams, is required to resolve the micro-slip of the system [8]. To investigate the effect of different seed distributions and corresponding mesh sizes on the QSMA results of the test structure, three models with different mesh configurations were tested. To evaluate the influence of these properties as independently as possible, all three models have the same parameters except varying settings in the mesh module. The coefficient of friction was set at 1.1 and the bolt preload at 2249 N for all models in this comparison.

The coarse mesh model has a total number of 9425 nodes defined by the user. Both the beam parts as well as the bolt assembly were meshed with a constant mesh density (uniform seeding) of 11 for the beams and three for the bolt assembly (see fig. 5.9 (a)).
The fine mesh model has a total number of 35763 nodes defined by the user. In this model, the beam parts were meshed based on biased seeding that gradually increased from three in the interface area to ten at the end of the beam. In addition, the number of elements in the depth direction of the beam was increased from one to two (see fig. 5.9 (b)). The bolt assembly was meshed with the same mesh density of three as for the coarse mesh model.
The super fine mesh model has a total number of 153535 nodes defined by the user. As with the fine mesh model, the beam parts were meshed based on biased seeding. The mesh density is gradually increased from two in the interface area to six at the end of the beam. The number of elements in the depth direction was increased to four (see fig. 5.9 (c)). The bolt assembly was meshed with a constant mesh density of 1.3.
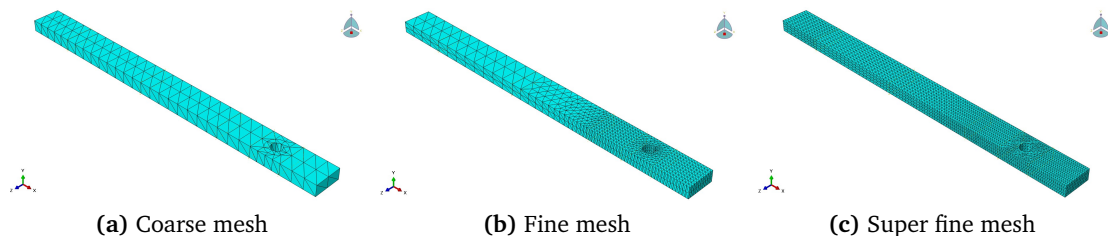

(a) Coarse mesh   **(b)** Fine mesh   **(c)** Super fine mesh

Figure 5.9: Different mesh configurations of the beam parts

Unfortunately, it was not possible to analyse the super fine mesh model with the computer

used to run all the simulations. Abaqus aborted the solving of the eigenproblem during the modal analysis step after several hours of computing due to a lack of ram. The coarse mesh model was investigated in the course of the QSMA routine for 20 uniformly distributed load amplitudes in the interval between 0 and 80000 (`alpha = np.linspace(0,80000,20)`. The fine mesh model was investigated for only 10 uniformly distributed load amplitudes in the same interval, because of its far more expensive simulations. The corresponding array was specified as `alpha = np.linspace(0,80000,10)`. Despite this difference, a comparison of the results can be made, since the number of load amplitudes in the interval does show only minor qualitatively significant differences in the results (see section 5.3.4). The total runtime of the QSMA routine was 23 min for the coarse mesh model and 98 min for the fine mesh model.

Based on the results of the two different mesh models, a strong influence of the mesh on the results of the QSMA routine can be observed. It can be seen that both the curves of the damping ratios and the curves of the natural frequencies show a strong difference for small modal amplitudes. As the modal amplitude increases, the curves of the two mesh models converge to the same slope. The damping ratios curves show an unexpected behaviour, since with increasing modal amplitude the damping ratios decrease after a certain maximum value. The reached maximum damping ratio of the fine mesh model is higher than the one of the coarse mesh model. In order to be able to make more precise statements about the reasons for this, further investigations must be carried out. In the course of that, a structured mesh convergence study should be carried out, as shown in [8].
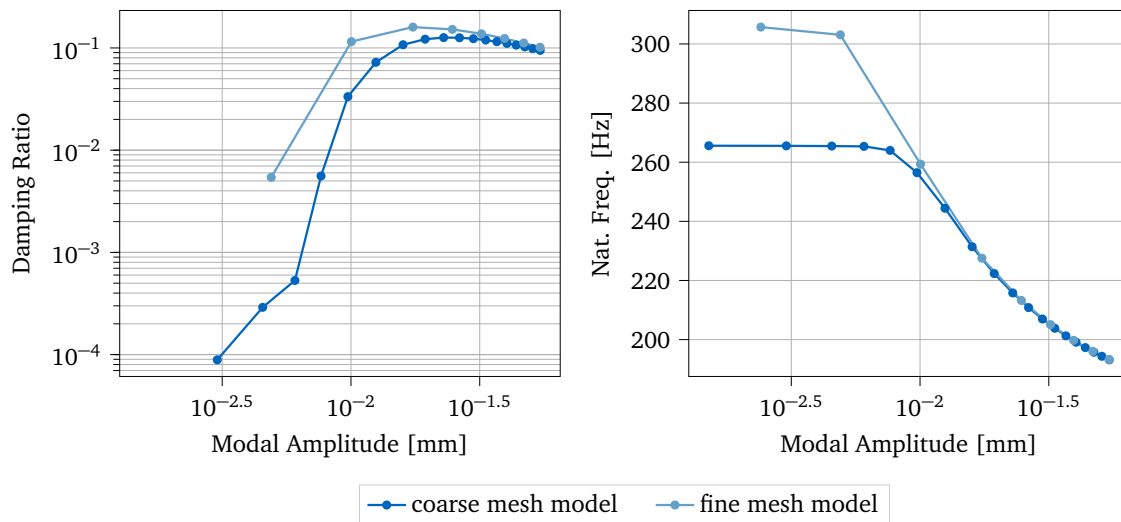

Figure 5.10: QSMA results - Influence of the mesh

5.3.2 Influence of the Friction Coefficient

The influence of the friction coefficient on the damping ratio and natural frequency resulting from the QSMA routine was investigated by analysing the coarse mesh model with the different friction coefficients 0.1, 0.3, 0.6, 1.1 and 1.6. The otherwise unchanged model was tested with a bolt preload of 2249 N for 10 uniformly distributed load amplitudes in the interval between 0 and 40000 (`alpha = np.linspace(0,40000,10)`).

The resulting curves of the damping ratio show the same counterintuitive behaviour as described in the section on the influence of the mesh. The fact that the damping ratio decreases after reaching a certain maximum can be observed for the test cases with a friction coeffi-
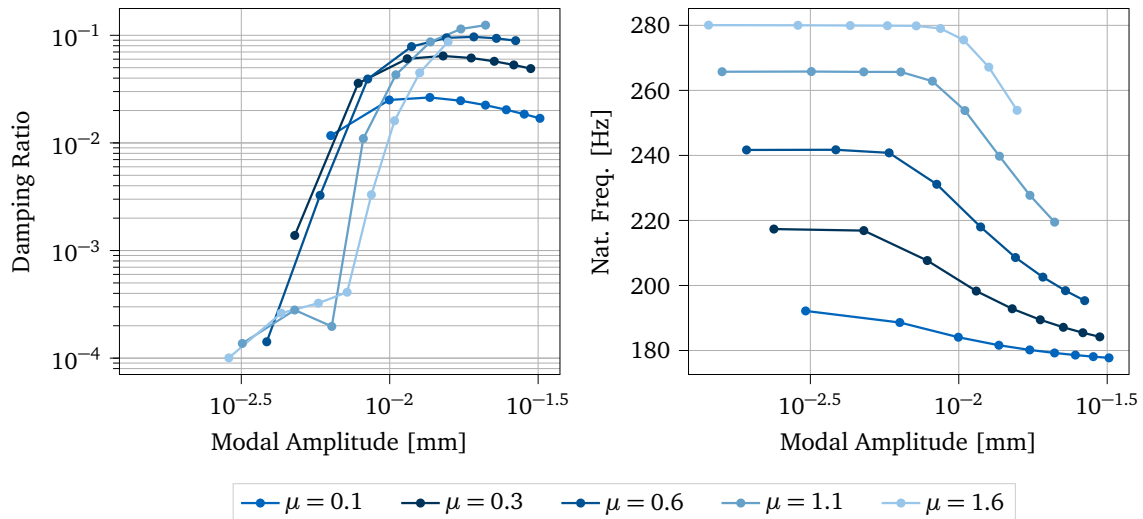
Figure 5.11: QSMA results - Influence of the friction coefficient

cient of 0.1, 0.3 and 0.6. It can be seen that the maximum damping ratio increases when the friction coefficient is also increased. In addition to these observations, it is assumed that an increase in the friction coefficient leads to a shift of the maximum damping ratio into the range of higher modal amplitudes. The resulting natural frequency curves show that as the coefficient of friction increases, the natural frequency of the structure also increases. It can also be observed that the slope of the frequency change also increases with an increasing friction coefficient.

5.3.3 Influence of the Bolt Preload

In order to qualitatively investigate the influence of the bolt preload on the results of the QSMA routine, the coarse mesh model was tested with three different preload forces. Apart from a varying bolt force amplitude, all model parameters were kept the same in the tests performed. All QSMA analyses were performed with a friction coefficient of 1.1. The load amplitude interval was set from 0 to 40000 with 40 evenly distributed load amplitudes for the lower preload forces and 20 load amplitudes for the highest preload force (reduction to reduce computational effort).

The two studies by Wall et al. [16] and Jewell et al. [8] show that a high degree of variation is required to match the results obtained with their QSMA routines with the corresponding experimental data. Since the required preload exceeds the maximum tensile strength of the bolt, it is assumed that there are non-modelled physical factors that need to be taken into account [16]. Based on these findings, it was decided to investigate the test structure with preload values of 2249 N, 5000 N and 80000 N to cover a wide range of load cases.

Due to an improvement of the curve fitting to obtain the linear relationship between preload and torque from the experimental data, the used preload value of 2249 N differs from the actual calculated value of 2238 N for the same torque of 10 Nm as shown in chapter 4. This improvement was made at a late stage of the project and should be taken into account in the further analysis of the system. However, due to the large uncertainty in the experimental bolt preload measurements, this marginal difference was neglected for the investigations listed here [16].

The resulting natural frequency curves show that with increasing bolt preload, the natural frequency of the structure increases and the total frequency change decreases (46.25 Hz for
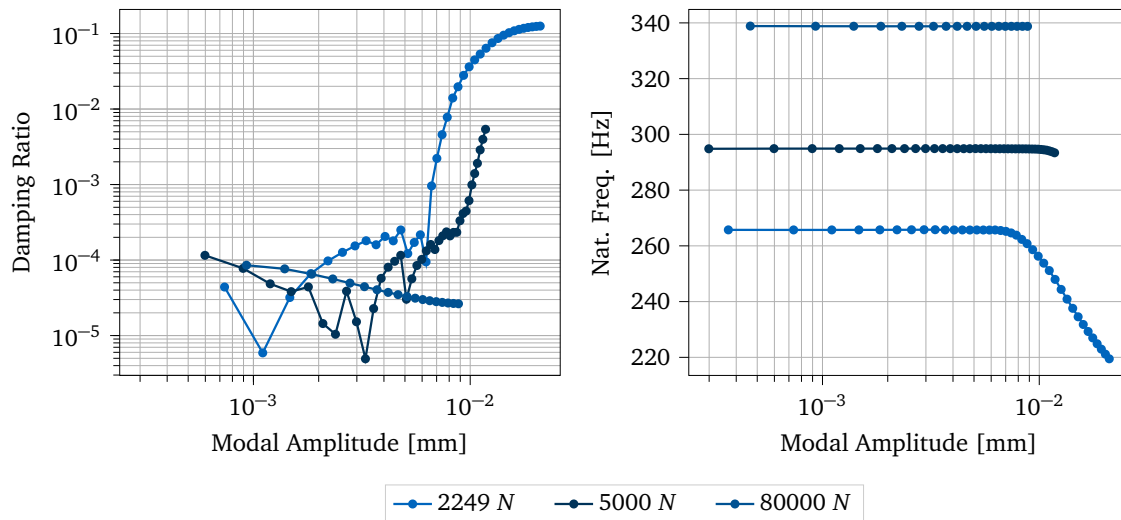
Figure 5.12: QSMA results - Influence of the bolt preload

2249 N, 1.49 Hz for 5000 N, 0.09 Hz for 80000 N). The resulting damping curves show that the general trend of a decreasing damping ratio with increasing preload found in [16] and [8] can be confirmed for higher modal amplitudes. This is to be expected as a lower preload would lead to more micro-slip in the joint and thus to a higher damping ratio [8]. However, is has to mentioned that the damping ratio slope, resulting from the model with a preload of 80000 N, shows an unexpected behaviour. The damping ratio decreases as the modal amplitude increases.

5.3.4 Influence of the Load Amplitude Interval

To investigate the effects of the load amplitude interval on the results of the QSMA routine, the coarse mesh model was tested with otherwise constant model parameters for two load arrays with different maximum load amplitudes. The test structure of the jointed beams was analysed for 20 uniformly distributed load amplitudes in the interval between 0 and 40000 (`alpha = np.linspace(0,40000,20)` and for 20 uniformly distributed load amplitudes in the interval between 0 and 80000 (`alpha = np.linspace(0,80000,20)`. Both QSMA analyses were performed with a friction coefficient of 1.1 and a bolt preload of 2249 N. As expected, a higher maximum amplitude of the load interval leads to a larger modal amplitude interval of the results. The plotted results (fig. 5.13) show that the curves of the damping ratio differ slightly for small modal amplitudes. In general, however, it can be said that both the damping ratio and the natural frequency curves have almost an identical shape. It seems as if the curves with the higher maximum load amplitude continue the curves with the lower maximum load amplitude. The counter-intuitive drop in the damping ratio from a certain modal amplitude value already mentioned can also be observed.

5.3.5 Influence of the Load Amplitude Density

In addition to the investigated effects of the maximum load amplitude on the QSMA results, the influence of the number of uniformly distributed load amplitudes is also investigated. The structure was tested for 10, 20 and 40 uniformly distributed load amplitudes in the interval between 0 and 40000. The corresponding load amplitude arrays are: `alpha`
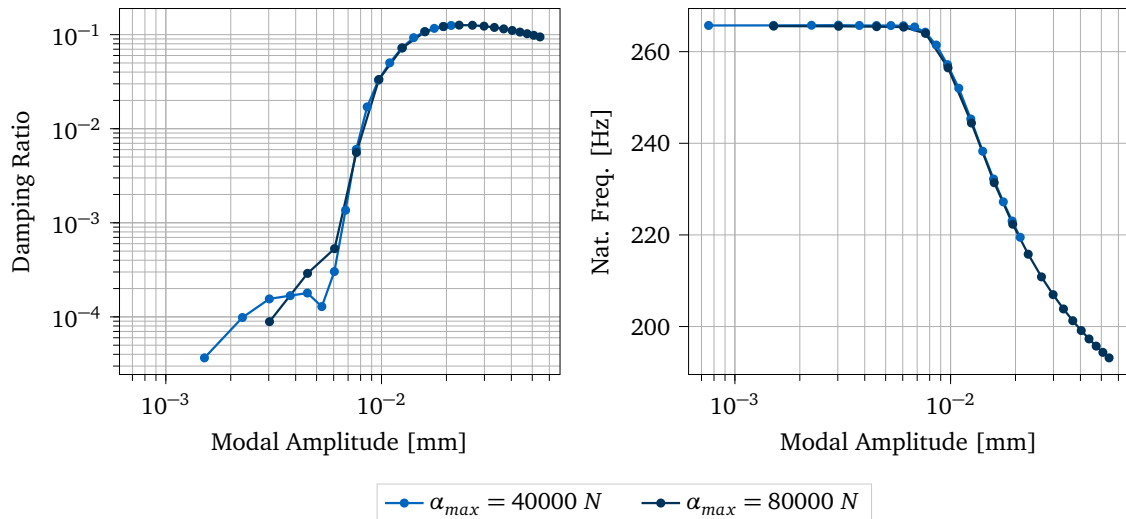
Figure 5.13: QSMA results - Influence of the load amplitude interval

= np.linspace(0,40000,10), alpha = np.linspace(0,40000,20) as well as alpha = np.linspace(0,40000,40). All three QSMA analyses were performed with the coarse mesh model, a friction coefficient of 1.1 and a bolt preload of 2249 N.
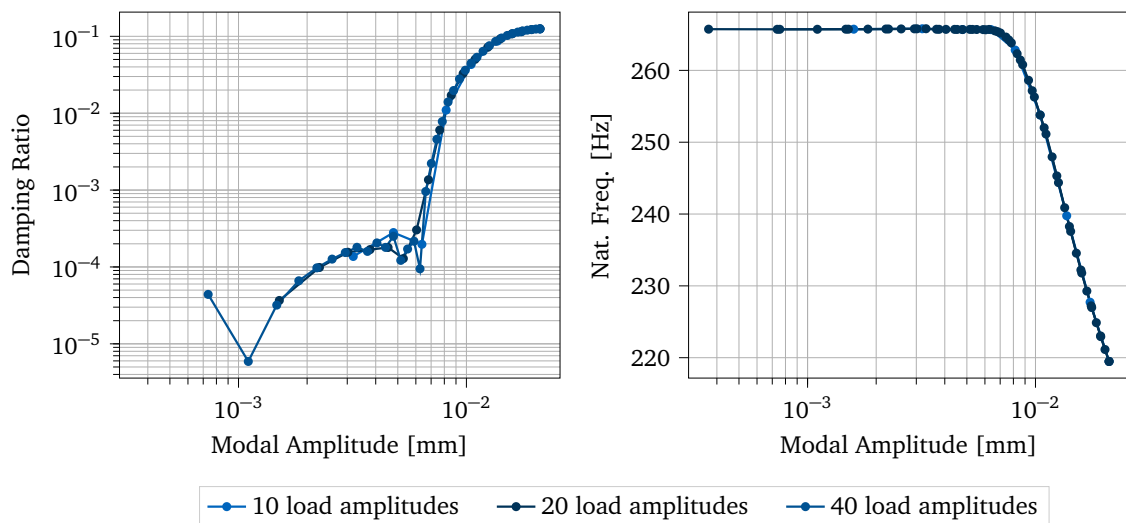

Figure 5.14: QSMA results - Influence of the load amplitude density

The resulting curves of the damping ratio and the natural frequency (fig. 5.14) show great similarities for all three test cases. The curves of the damping ratios show an unexpected step-like progression. In the middle range of the modal amplitude, where the slope of the damping ratio curve decreases, the curves of the different test cases differ most. It can be seen that in general a higher load amplitude density leads to a smoother slope (especially for the damping ratio curves). The fact that the force density does not significantly affect the qualitative trend of the QSMA results was helpful as it was possible to perform parameter studies with less load amplitudes and still obtain useful results. This led to a reduction in the overall run time of the routine, which was particularly helpful in the experiments with the fine mesh model. The total running time of the QSMA routine was 11 minutes for 10, 21 minutes for 20 and 39 minutes for 40 load amplitudes.

5.3.6 Influence of Loading the Bolt Assembly

To check whether the loading of the bolt assembly affects the QSMA results, a special function was implemented in the routine that allows all nodes of the bolt assembly to be excluded from the loading. Further details about the exact implementation can be found in chapter 2. The coarse mesh model was analysed for two different routine settings. The results of the QSMA run with a loaded bolt assembly servse as a reference for comparing the results of the run without a loaded bolt assembly. Apart from these differences, all other model parameters and routine settings were kept. The model was analysed with a friction coefficient of 1.1, a given preload of 2249 N and the load amplitude interval `alpha = np.linspace(0,40000,20)` for both runs.
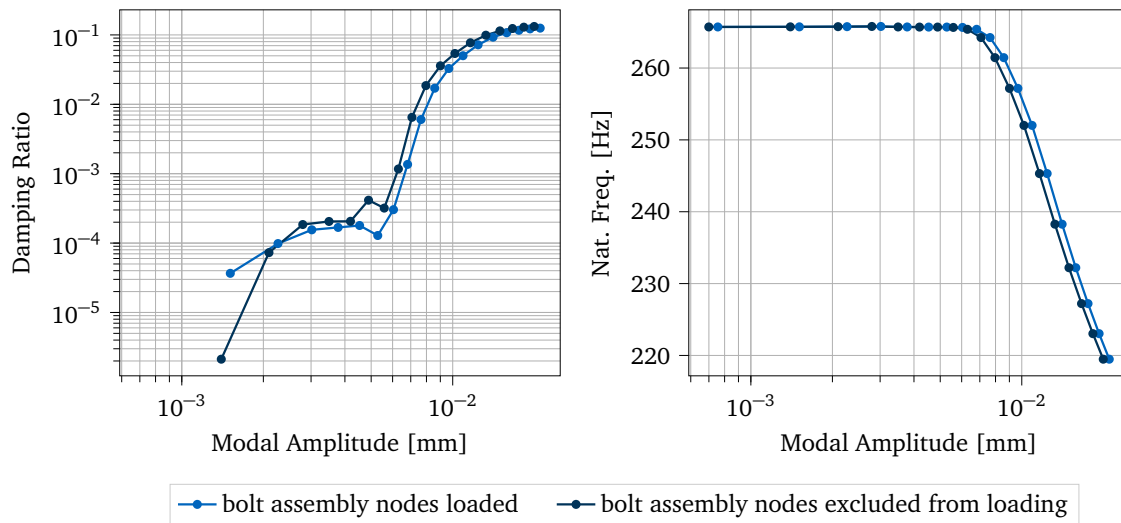

Figure 5.15: QSMA results - Influence of loading the bolt assembly

The resulting damping ratio curves show the same step-like progression and have almost exactly the same curve shape. The curves differ most in the middle range of the modal amplitude, where the slope of the damping ratio decreases. It appears that excluding the bolt assembly from the loading results in slightly higher damping ratios than the system with the bolt assembly loaded. Another result is that both natural frequency curves have the same shape. It seems that the exclusion of the bolt assembly from the loading leads to a slight shift of the curve towards lower modal amplitudes compared to the system with the bolt assembly loaded. In summary, the results show that the loading of the bolt assembly does not have a great influence on the QSMA results.

5.3.7 Influence of the Interpolation During the Evaluation

In this section, the influence of the number of data points of the modal load and displacement data on the instantaneous damping ratios and natural frequencies is shown. For this purpose, the modal load-displacement data obtained by analysing the coarse mesh model with a friction coefficient of 1.1, a given preload of 2249 N and the load amplitude interval `alpha = np.linspace(0,40000,20)` were evaluated with two different function settings. The evaluation without interpolation served as a reference for the evaluation with interpolation. Using the interpolation for the evaluation, the modal displacement is fitted as a function of the load amplitude for 100 points (default value). This fitting is done before the hysteresis curve is constructed and the instantaneous natural frequencies and damping ratios are calculated.
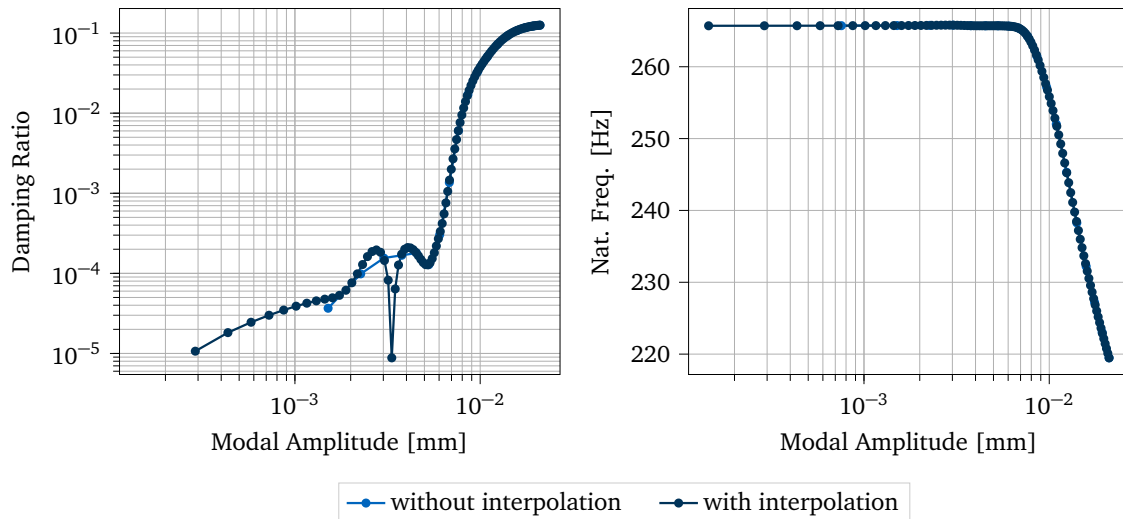
Figure 5.16: QSMA results - Influence of the interpolation during the evaluation

Looking at the resulting damping ratio curves of the analyses, one can see that the curve shapes matches particularly well for higher modal amplitudes. The biggest difference of the resulting damping ratio curves can be seen in the middle range of the modal amplitude. The damping ratio curve, resulting from the evaluation with interpolation, shows an unexpectedly strong drop of the damping in this range. The representation of the drop is reinforced by the logarithmic scaling of the plot. It is assumed that this unusualness is due to errors in the computation of the dissipated energy per corresponding loading cycle with the trapezoidal rule. The resulting natural frequency curves both show the same shape and no significant difference can be seen. In general, one can say that the interpolation leads to a smoother slope of the resulting damping ratio and natural frequency curves.

Chapter 6

Conclusion and Future Work

The implementation and functionality of the QSMA routine developed in this work has been described in detail. Particular attention was paid to the processing of the results issued by Abaqus. The design of the Brake-Reuß beam variant was presented and the experiments for determining the preload-torque relationship and the impact hammer tests were covered. These obtained results where then used to evaluated the functionality of the QSMA routine. To address the problem of unstable results, due to rigid-body modes in the analysis of the free-free model of the test structure, three different stabilization approaches were tested and evaluated against experimental data.

The investigations showed that interia relief as used by Wall et al. [16] is not applicable for this type of analysis, which is in agreement with the Abaqus documentation.

The method of using springs attached to the test structure and connected to the ground to constrain the rigid body motion was tested in various spring assembly configurations. The number of springs, the attachment positions and the spring stiffness were varied. The configuration was found to have a strong influence on the convergence of the results. From all tests, a configuration with eight spring assemblies led to the most promising QSMA results. In this case, the obtained curves of the damping ratio correspond to the shape of the experimental damping ratio curve with a high material damping value. However, the natural frequency curve could not be similarly matched.

The effectiveness of the automatic stabilization mechanism (automatic addition of volume proportional damping) provided by Abaqus was also evaluated for different settings. It was found that the QSMA results with the mechanism in its default configuration almost exactly matched the results of the system with the eight-spring-assembly configuration. The stabilization mechanism was used for function validation of the QSMA routine due to its lower implementation effort and lower configuration dependency compared to the spring configuration method. In the course of this, a modified FE model of the test structure was analyzed in free-free configuration. The contact at the interface between the beams of this model was replaced by a tie constraint. The results of the QSMA analyses were consistent with the expected linear behaviour of the structure, validating its functionality. However, it was also found that the damping caused by the stabilization mechanism affects the QSMA results. For this reason, further investigations are required to assess whether this mechanism can be used in the analysis of a FE model with an implemented contact formulation without distorting the results.

The performed QSMA analyses of the boundary condition model allowed to evaluate the effects of certain FE model parameters and QSMA routine settings on the analysis results by eliminating the problems related to the singularity of the free-free test model. It was found that the mesh density, the friction coefficient and the bolt preload all strongly influence the QSMA results. In contrast, it was possible to show that the load amplitude interval, the load

amplitude density, the loading of the bolt assembly and the interpolation during the evaluation have a minor and subordinate influence on the QSMA results.

Since the focus of this thesis was mainly on the functional implementation of the QSMA routine and the investigation of the stability problem, the investigation on the influence of model parameters and routine settings was limited. Future work on this topic should aim to investigate the interface conditions and surface contours of the joined beams since they also affect the response of the system [8, 16]. Furthermore, the influence of the material parameters and the solver settings can be taken into account when trying to reconcile the QSMA results with the experimental data.

In addition to a more detailed parameter study, the effect of evaluating the damping ratios as well as the natural frequencies at peak modal amplitude values instead of modal amplitude values should be investigated. The peak modal amplitude is obtained by multiplying the modal amplitude by the peak value of the mode shape. This approach is similarly implemented in other studies [8, 16] and could lead to greater agreement between experimental data and QSMA results.

Bibliography

[1]   Allen, M. S., Lacayo, R. M., and Brake, M. R. W. "Quasi-static Modal Analysis based on Implicit Condensation for Structures with Nonlinear Joints". In: 2016.

[2]   Ames, N. M., Lauffer, J. P., Jew, M. D., Segalman, D. J., Gregory, D. L., Starr, M. J., and Resor, B. R. "Handbook on dynamics of jointed structures." In: (July 2009). DOI: 10.2172/1028891.

[3]   Bäker, M. "How to get meaningful and correct results from your finite element model". preprint. Nov. 2018.

[4]   Brake, M. R. W. and Reuß, P. "The Brake-Reuß Beams: A System Designed for the Measurements and Modeling of Variability and Repeatability of Jointed Structures with Frictional Interfaces". In: *The Mechanics of Jointed Structures*. Springer International Publishing, July 2017, pp. 99–107. DOI: 10.1007/978-3-319-56818-8_9. URL: https://doi.org/10.1007/978-3-319-56818-8_9.

[5]   Fantetti, A. "Testing-based Parametrization of Contact and Friction - Early Stage Assessment". In: (2018).

[6]   Festjens, H., Chevallier, G., and Dion, J.-l. "A numerical tool for the design of assembled structures under dynamic loads". In: *International Journal of Mechanical Sciences* 75 (2013), pp. 170–177. ISSN: 0020-7403. DOI: https://doi.org/10.1016/j.ijmecsci.2013.06.013. URL: https://www.sciencedirect.com/science/article/pii/S0020740313001860.

[7]   *Inertia relief*. Accessed: 2022-03-09. URL: https://abaqus.uclouvain.be/English/SIMACAEANLRefMap/simaanl-c-inertiarelief.htm.

[8]   Jewell, E., Allen, M. S., Zare, I., and Wall, M. "Application of quasi-static modal analysis to a finite element model and experimental correlation". In: *Journal of Sound and Vibration* 479 (2020), p. 115376. ISSN: 0022-460X. DOI: https://doi.org/10.1016/j.jsv.2020.115376. URL: https://www.sciencedirect.com/science/article/pii/S0022460X20302078.

[9]   Klöcker, M. and Westphal, S. "Investigations of friction-relevant parameters to ensure reliable bolted joints". In: *MATEC Web of Conferences* 94 (2017). Ed. by Oancea, G. and Drăgoi, M., p. 04007. DOI: 10.1051/matecconf/20179404007. URL: https://doi.org/10.1051/matecconf/20179404007.

[10]   Lacayo, R. M. and Allen, M. S. "Updating structural models containing nonlinear Iwan joints using quasi-static modal analysis". In: *Mechanical Systems and Signal Processing* 118 (2019), pp. 133–157. ISSN: 0888-3270. DOI: https://doi.org/10.1016/j.ymssp.2018.08.034. URL: https://www.sciencedirect.com/science/article/pii/S0888327018305739.

[11]   Lengger, M. and Willner, K. "Application of Quasi-static Modal Analysis to the Tribomechadynamics Benchmark System". In: (2021).

[12]   NASA. *REQUIREMENTS FOR THREADED FASTENING SYSTEMS IN SPACEFLIGHT HARD-WARE, NASA-STD-5020A*. Approved: 2018-09-04 Superseding NASA-STD-5020 (Baseline). 2018.

[13]   Niemann, G., Winter, H., Höhn, B.-R., and Stahl, K. *Maschinenelemente 1*. Springer Berlin Heidelberg, 2019. DOI: 10.1007/978-3-662-55482-1. URL: https://doi.org/10.1007/978-3-662-55482-1.

[14]   Smith, S. A., Catalfamo, S., Bilbao-Ludena, J. C., Brake, M. R. W., Reuß, P., and Schwingshackl, C. W. "Considerations for Measurements of Jointed Structures". In: *The Mechanics of Jointed Structures*. Springer International Publishing, July 2017, pp. 109–133. DOI: 10.1007/978-3-319-56818-8_10. URL: https://doi.org/10.1007/978-3-319-56818-8_10.

[15]   *Solving nonlinear problems*. Accessed: 2022-03-011. URL: https://abaqus-docs.mit.edu/2017/English/SIMACAEANLRefMap/simaanl-c-nonlineareqns.htm.

[16]   Wall, M., Allen, M. S., and Zare, I. "Predicting S4 Beam Joint Nonlinearity Using Quasi-Static Modal Analysis". In: *Nonlinear Structures and Systems, Volume 1*. Ed. by Kerschen, G., Brake, M. R. W., and Renson, L. Cham: Springer International Publishing, 2020, pp. 39–51. ISBN: 978-3-030-12391-8.

[17]   Wang, Y., Ma, Y., Hong, J., Battiato, G., and Firrone, C. M. "A Novel Test Rig for the Basic Nonlinear Characterization of Bolted Joints". In: *Applied Sciences* 11.12 (2021). ISSN: 2076-3417. DOI: 10.3390/app11125613. URL: https://www.mdpi.com/2076-3417/11/12/5613.

[18]   Zare, I. and Allen, M. S. "Adapting a contact-mechanics algorithm to predict damping in bolted joints using quasi-static modal analysis". In: *International Journal of Mechanical Sciences* 189 (Jan. 2021), p. 105982. DOI: 10.1016/j.ijmecsci.2020.105982. URL: https://doi.org/10.1016/j.ijmecsci.2020.105982.

Disclaimer

I hereby declare that this thesis is entirely the result of my own work except where otherwise
indicated. I have only used the resources given in the list of references.

Garching bei München, March 28, 2022

_____
(Signature)